Since January 2020 Elsevier has created a COVID-19 resource centre with free information in English and Mandarin on the novel coronavirus COVID-19. The COVID-19 resource centre is hosted on Elsevier Connect, the company's public news and information website.

Science of the Total Environment 823 (2022) 153720

Contents lists available at ScienceDirect

Science of the Total Environment

journal homepage: www.elsevier.com/locate/scitotenv

Decrease in ambient volatile organic compounds during the COVID-19 lockdown period in the Pearl River Delta region, south China

Chenglei Pei [a,b,e], Weiqiang Yang [a,g], Yanli Zhang [a,c,d], Wei Song [a], Shaoxuan Xiao [a,d,e], Jun Wang [a,d,e], Jinpu Zhang [a,b,e], Tao Zhang [f], Duohong Chen [f], Yujun Wang [b], Yanning Chen [b], Xinming Wang [a,c,d,e,*]

[a] State Key Laboratory of Organic Geochemistry, Guangdong Key Laboratory of Environmental Protection and Resources Utilization, Guangzhou Institute of Geochemistry, Chinese Academy of Sciences, Guangzhou 510640, China
[b] Guangzhou Sub-branch of Guangdong Ecological and Environmental Monitoring Center, Guangzhou 510060, China
[c] Center for Excellence in Regional Atmospheric Environment, Institute of Urban Environment, Chinese Academy of Sciences, Xiamen 361021, China
[d] CAS Center for Excellence in Deep Earth Science, Guangzhou 510640, China
[e] University of Chinese Academy of Sciences, Beijing 100049, China
[f] State Environmental Protection Key Laboratory of Regional Air Quality Monitoring, Guangdong Ecological and Environmental Monitoring Center, Guangzhou 510308, China
[g] Guangdong Provincial Academy of Environmental Sciences, Guangzhou 510045, China

HIGHLIGHTS

- MDA8-O_3, NOx, and VOCs decreased by 11%, 57% and 19% during the lockdown than before.
- More reactive alkenes and aromatics showed larger decrease rates than alkanes during the lockdown.
- Higher alkanes (C ≥ 6) decreased much more than lighter alkanes (C < 6) during the lockdown.
- Industrial and diesel-engine emission reductions largely explain the decreased VOCs during the lockdown.

GRAPHICAL ABSTRACT

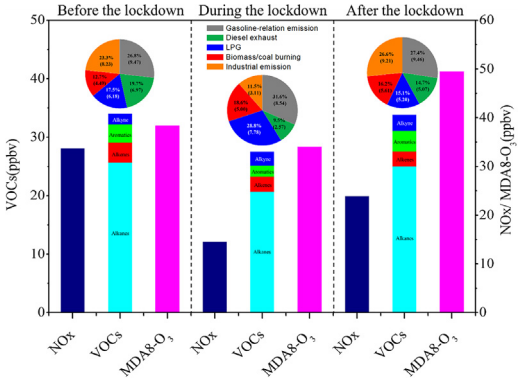

ARTICLE INFO

Article history:
Received 22 December 2021
Received in revised form 30 January 2022
Accepted 3 February 2022
Available online 8 February 2022

Editor: Jianmin Chen

Keywords:
COVID-19
Volatile organic compounds
Ozone
NOx
PRD

ABSTRACT

During the COVID-19 lockdown, ambient ozone levels are widely reported to show much smaller decreases or even dramatical increases under substantially reduced precursor NOx levels, yet changes in ambient precursor volatile organic compounds (VOCs) have been scarcely reported during the COVID-19 lockdown, which is an opportunity to examine the impacts of dramatically changing anthropogenic emissions on ambient VOC levels in megacities where ozone formation is largely VOC-limited. In this study, ambient VOCs were monitored online at an urban site in Guangzhou in the Pearl River Delta region before, during, and after the COVID-19 lockdown. The average total mixing ratios of VOCs became 19.1% lower during the lockdown than before, and those of alkanes, alkenes and aromatics decreased by 19.0%, 24.8% and 38.2%, respectively. The levels of light alkanes (C < 6) decreased by only 13.0%, while those of higher alkanes (C ≥ 6) decreased by 67.8% during the lockdown. Disappeared peak VOC levels in morning rush hours and the drop in toluene to benzene ratios during the lockdown suggested significant reductions in vehicle exhaust and industrial solvent emissions. Source apportioning by positive matrix factorization model revealed that reductions in industrial emissions, diesel exhaust (on-road diesel vehicles and off-road diesel engines) and gasoline-related emissions could account for 48.9%, 42.2% and 8.8%, respectively, of the decreased VOC levels during the lockdown.

* Corresponding author at: State Key Laboratory of Organic Geochemistry, Guangdong Key Laboratory of Environmental Protection and Resources Utilization, Guangzhou Institute of Geochemistry, Chinese Academy of Sciences, Guangzhou 510640, China.
E-mail address: wangxm@gig.ac.cn (X. Wang).

http://dx.doi.org/10.1016/j.scitotenv.2022.153720

Moreover, the reduction in industrial emissions could explain 56.0% and 70.0% of the reductions in ambient levels of reactive alkenes and aromatics, respectively. An average increase in O_3–1 h by 17% and a decrease in the daily maximum 8-h average ozone by 11% under an average decrease in NOx by 57.0% and a decrease in VOCs by 19.1% during the lockdown demonstrated that controlling emissions of precursors VOCs and NOx to prevent ambient O_3 pollution in megacities such as Guangzhou remains a highly challenging task.

1. Introduction

Volatile organic compounds (VOCs), as important precursors of ozone (O_3) and secondary organic aerosols (SOA) (Atkinson, 2000; Chameides et al., 1992; Forstner et al., 1997; Odum et al., 1997; O'Dowd et al., 2002; Sato et al., 2010), play an important role in photochemical smog and fine particle pollution. SOA account for a substantial part of ambient fine particles, particularly during haze events (Guo et al., 2014; Huang et al., 2014; Zhang et al., 2014), and O_3 production is often in the VOC-limit regime, particularly in densely populated urban areas (Ding et al., 2013; Jin and Holloway, 2015; Tie et al., 2013). Therefore, emission control of anthropogenic VOCs has increasingly become a priority for the coordinated control of $PM_{2.5}$ and O_3 pollution (Xu et al., 2016). However, due to the huge diversity in VOC emission sources, composition profiles, atmospheric reactivities and air quality impacts, formulating control strategies for VOCs is a highly challenging task, especially in megacities.

Although sound control policy-making for VOCs relies heavily on emission inventories, particularly emission inventories for more reactive VOC species, this effort is often frustrated both by the lack of in-time quality source profiles and emission factors and by the uncertainties in activity levels. Alternatively, the effectiveness of control measures could be evaluated or confirmed by tracking the changes in ambient levels of air pollutants after short-term proactive intervention measures were adopted for good air quality during internationally or nationally important events such as the 2008 financial crisis (Monteiro et al., 2018; Zhang et al., 2012), the 2010 Asian Games (Huang et al., 2017, 2020; Liu et al., 2013), the 2014 Asia-Pacific Economic Cooperation (APEC) summit (Li et al., 2015; Yang et al., 2018) and the 2015 China Victory Day Parade (Li et al., 2016). Valuable implications can also be obtained by tracing changing air quality during long holidays with passive emission reduction, e.g., in industry sectors (Wang et al., 2021a, 2021b).

After the outbreak of the COVID-19 pandemic, many countries are locking their population and enforcing strict quarantine to control the spread of the havoc of this highly communicable disease. Apart from the daily life of citizens, various industries and sectors are heavily affected; therefore, emissions of air pollutants are passively reduced, especially during lockdown intervals with largely halted traffic and factory production (Chen et al., 2020a; Lian et al., 2020; Lal et al., 2020; Marlier et al., 2020). This opens a window to look at air quality impacts of changing anthropogenic emissions at a scale that cannot be normally achieved (Chen et al., 2020b; Cui et al., 2020; Wang et al., 2020a). One distinctive change in air quality during the pandemic lockdown is that concentrations of O_3 did not decrease at similar scales or even increase as other air pollutants dropped dramatically. According to observation data obtained from the China National Environmental Monitoring Center, while concentrations of $PM_{2.5}$, NO_2, SO_2 and CO in China during the COVID-19 pandemic in early 2020 decreased by 19%, 30%, 21% and 14%, respectively, when compared to their levels in 2019 (Chu et al., 2021), concentrations of O_3 instead demonstrated a notable increase (12%). Studies based surface monitoring and satellite observations also revealed that O_3 levels increased during COVID-19 lockdown while levels of NOx and $PM_{2.5}$ decreased (Huang et al., 2021; Miyazaki et al., 2020; Wang and Zhang, 2020). Moreover, several periods of heavy haze pollution still occurred in eastern China despite large decreases in primary pollution during the lockdown (Chen et al., 2020b). Using satellite data and a network of >10,000 air quality stations and after accounting for the effects of meteorological variability, Venter et al. (2020) found that lockdown events reduced the population-weighted concentrations of NO_2 and $PM_{2.5}$ by approximately 60% and 31%, respectively, with a marginal increase in O_3 by approximately 4% in 34 countries during lockdown dates up until May 15th, 2020. The unexpected occurrence of $PM_{2.5}$ pollution and haze events in northern and eastern China (Huang et al., 2021; Lv et al., 2020; Wang et al., 2020b) and the wide-range increase in O_3 concentration (Chu et al., 2021; Miyazaki et al., 2020; Wang et al., 2020a; Wang and Zhang, 2020) during the COVID-19 lockdown with unprecedented emission reduction demonstrate difficulties in the coordinated control of $PM_{2.5}$ and O_3.

Similar to the spatial variability in the complex O_3 − VOC − NOx relationships (Jin and Holloway, 2015), the responses of ambient O_3 to the lockdown measures showed great regional disparities. By combining observational data and model simulations, Wang et al. (2021c) found that although there was a noticeable drop in primary pollutants in both the Yangtze River Delta region (YRD) and Pearl River Delta region (PRD) in China, the maximum daily 8 h average O_3 (MDA8-O_3) soared by 20.6–76.8% in the YRD but decreased by 15.5–28.1% in the PRD. More specifically, based on model studies $PM_{2.5}$, NO_2, and SO_2 were estimated decreased significantly while O_3 would have no obvious change or even increase greatly in the PRD and YRD regions (Li et al., 2020b; Wang et al., 2021d). While O_3 and NOx data can be obtained in a large number of air quality monitoring stations with high time resolution, the lack of high time resolution monitoring data of VOCs is a bottleneck to understand the spatial variability in the O_3 − VOCs − NOx relationships.

The reduction in VOCs during lockdowns could be assessed by modeling (Guevara et al., 2021; Doumbia et al., 2021; Lv et al., 2020) or indicated by tropospheric HCHO vertical column densities from remote sensing (Pei et al., 2020). However, ambient monitoring of speciated VOCs would reflect the changes more straightforwardly and precisely. Although there are apparent differences between the PRD and the YRD in changing O_3 due to the COVID-19 lockdown (Wang et al., 2021c), until the present there were only a few reports about changes in the ambient levels and compositions of VOCs during the lockdown in the YRD (Jia et al., 2020; Wang et al., 2021c), and only one study was available with an observation-based approach in the evaluation of O_3 production to precursor changes during the COVID-19 lockdown in Dongguan city in the PRD (Qi et al., 2021). In the YRD, monitoring in the megacity Shanghai during a one-month non-control period and the following one-month COVID-19 outbreak control period revealed an average VOC reduction rate of 38.9% at the urban supersite and of 50.7% at the regional supersite due largely to decreased contributions from vehicle exhaust and fugitive emissions from the petrochemical industry (Jia et al., 2020). In another megacity Nanjing in the YRD, Wang et al. (2021e) observed a VOC reduction rate of 47% due to COVID-19 outbreak control and even larger reduction rates (49%–92%) for the more reactive aromatics and alkenes, which are relatively more important precursors of O_3 and SOA.

In this study, VOC species were measured online with a 1-h resolution from January 13th to March 15th, 2020 at an urban site in the megacity Guangzhou in the PRD. The changes in mixing ratios, compositions and diurnal variations of VOCs, as well as their sources and O_3/SOA formation potentials, during the lockdown (January 24th to February 16th, 2020) were compared with those before and after the lockdown. As O_3 pollution has shown a worsening trend in China's major urban centers (Li et al., 2020a; Lu et al., 2020) and O_3 formation in these urban centers is largely VOC-limited (Jin and Holloway, 2015; Wu and Xie, 2017), investigating the changing ambient VOCs with unprecedented passive emission reduction due to the COVID-19 lockdown would yield very useful implications in grappling with O_3 pollution problems in China's urban centers.

2. Experimental

2.1. Field measurements

Online measurements of VOCs were conducted approximately 23 m above ground at the rooftop of the eight-story building of the Guangzhou Environmental Monitoring Center (GEMC; 23.13°N, 113.27°E; Fig. 1), which is a state-controlled station in the national air quality monitoring network of China. The site is surrounded by residential, commercial and office buildings without any industrial emission sources but with dense traffic in the neighborhood (Fig. 1).

VOCs were measured online from January 13th, 2020 to March 15th, 2020, covering the periods before (January 13th - 23rd; Period I), during (January 24th - February 16th; Period II), and after (February 17th - March 15th) the COVID-19 lockdown forced by Guangdong Province with a series of measures implemented to prevent the spread of the pandemic (Table S1; Fig. S1).

A total of 55 hydrocarbon species (28 alkanes, 10 alkenes, 16 aromatics and ethyne) were measured once an hour using an online system (GC-866; Chromatotec Inc., France) including two separate high-performance gas chromatograph-flame ionization detectors (GC-FID) with online sample preparation. Detailed information about the instrument is described elsewhere (Pei et al., 2021). Briefly, one GC-FID (airmoVOC C_2-C_6) was used to analyze C_2-C_6 compounds, and another GC-FID (airmoVOC C_6-C_{12}) was used to analyze C_6-C_{12} compounds with varied sampling volumes and trapping conditions. The trapped VOCs were thermally desorbed and transferred to GC-FID, where they were separated by analytical columns and detected by FID. The C_2-C_6 VOCs were separated by an ultimetal column (PLOT Al_2O_3/Na_2SO_4, 25 m × 0.55 mm I.D. × 10 μm film thickness; Agilent, USA) with hydrogen as the carrier gas. The GC oven temperature was set to first increase from 36 °C to 38 °C in 1 min and then at 15 °C/min to 202 °C with a final holding time of 10.5 min. For the analysis of C_6-C_{12} hydrocarbons, a capillary metallic column (MXT30 CE; 30 m × 0.28 mm I.D. × 1.0 μm film thickness) was used for separation and the oven temperature was programmed to be initially 36 °C, increase at 2 °C/min to 50 °C, then at 10 °C/min to 80 °C, and then at 15 °C/min to 200 °C with a holding time of 6 min.

2.2. Quality assurance and quality control

During the campaign, the instrument was externally calibrated by diluting the PAMS standard (1 ppmv; Spectra Gases Inc., New Jersey, USA) to concentrations of 0.5, 2, 4, 6, 8, and 10 ppbv and running the five standards and zero air the same way as ambient air samples to obtain the calibration curves. Target compounds were identified based on their retention times. Each week, the system was challenged by one-point (4 ppbv) calibration, and recalibration was needed if the responses of C_2-C_{12} species were beyond ±15% of the calibration curves. The method detection limits (MDLs) for target VOC species are presented in Table S2.

2.3. Meteorological parameters and other air pollutants

The temperature (T), atmospheric pressure (P), relative humidity (RH), wind speed (WS) and wind direction (WD) were monitored simultaneously with an automatic weather station at GEMC. The planetary boundary layer higher (PBL) was computed through NOAA's READY Archived Meteorology website (http://www.ready.noaa.gov/READYamet.php; last access: 23 January 2021) every 3 h during the campaign.

CO, NO_x, O_3, and SO_2 were all monitored online with Model 48i, Model 42i, Model 49i, and Model 43i analyzers (Thermo Fisher Scientific, USA), respectively. PM_{10} and $PM_{2.5}$ were monitored by a Model 5030i Synchronized Hybrid Ambient Real-time Particulate analyzer (Thermo Fisher Scientific, USA).

2.4. Positive Matrix Factorization (PMF)

Sources of VOCs were explored using the USEPA Positive Matrix Factorization (PMF) model (version 5.0) with inputs of VOC monitoring data and uncertainties associated with the data. Data values below the MDL were substituted with MDL/2; missing data values were substituted with median concentrations. If the concentration is less than or equal to the MDL provided, the uncertainty is calculated as Unc = 5/6 × MDL; and if the concentration is greater than the MDL provided, the uncertainty is calculated

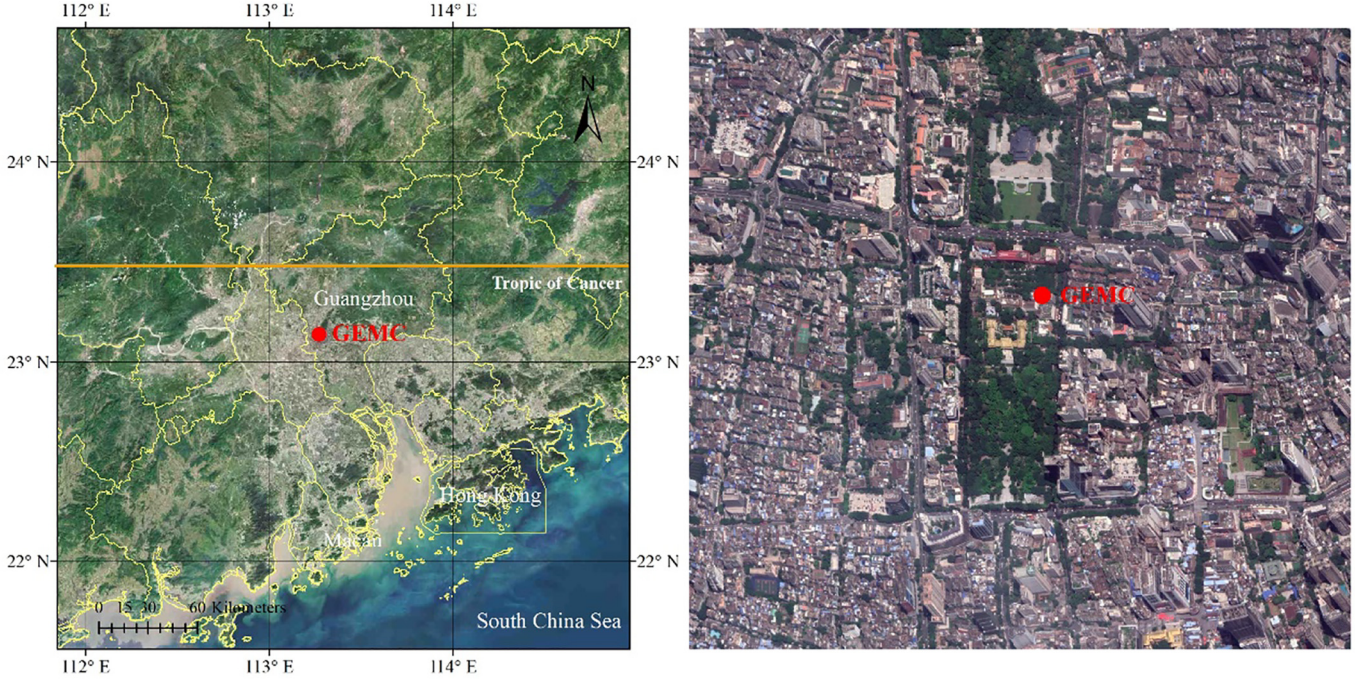

Fig. 1. Maps showing the location of the observation station (Guangzhou Environmental Monitoring Center, GEMC) in the Pearl River Delta region in south China (left; modified from the map drawn with ArcGIS Desktop version 10.0, ESRI, Redlands, CA, USA; http://www.esri.com) and the layout of the station's surroundings in urban Guangzhou (right; modified from Google Earth photo).

as Unc = [(error faction × mixing ratio)^2 + (MDL)^2]$^{1/2}$, where an error faction of 0.2 is used in this study.

3. Results and discussion

3.1. Overview of changing air quality during the COVID-19 lockdown

Fig. 2 shows the time series of $PM_{2.5}$, NO, NO_2, CO, SO_2, O_3, and total VOCs and their group compositions during the field campaign. On average, PM_{10} dropped from 50 μg/m^3 before the lockdown (Period I) to 28 μg/m^3 during the lockdown (Period II) and increased again to 40 μg/m^3 after the lockdown (Period III), while $PM_{2.5}$ decreased from 28 μg/m^3 before the lockdown to 21 μg/m^3 during the lockdown (Table 1). Similarly, CO and SO_2 decreased by 32% and 21%, respectively, and more pronounced declines were observed for NO and NO_2, which dropped by 63% and 56% in Period II when compared to those in Period I. Since CO, NOx and SO_2 are primary air pollutants largely related to combustion emissions (e.g., vehicles) (Bian et al., 2019; Cai et al., 2018; Chang et al., 2009; Li et al., 2017; Wang et al., 2002a; Xue et al., 2016), the decreases in their ambient levels reflect the changing activity levels particularly in industry and transportation sectors during the lockdown. After the lockdown (Period III), PM_{10}, $PM_{2.5}$, NO, NO_2, CO, and SO_2 all reasonably increased by

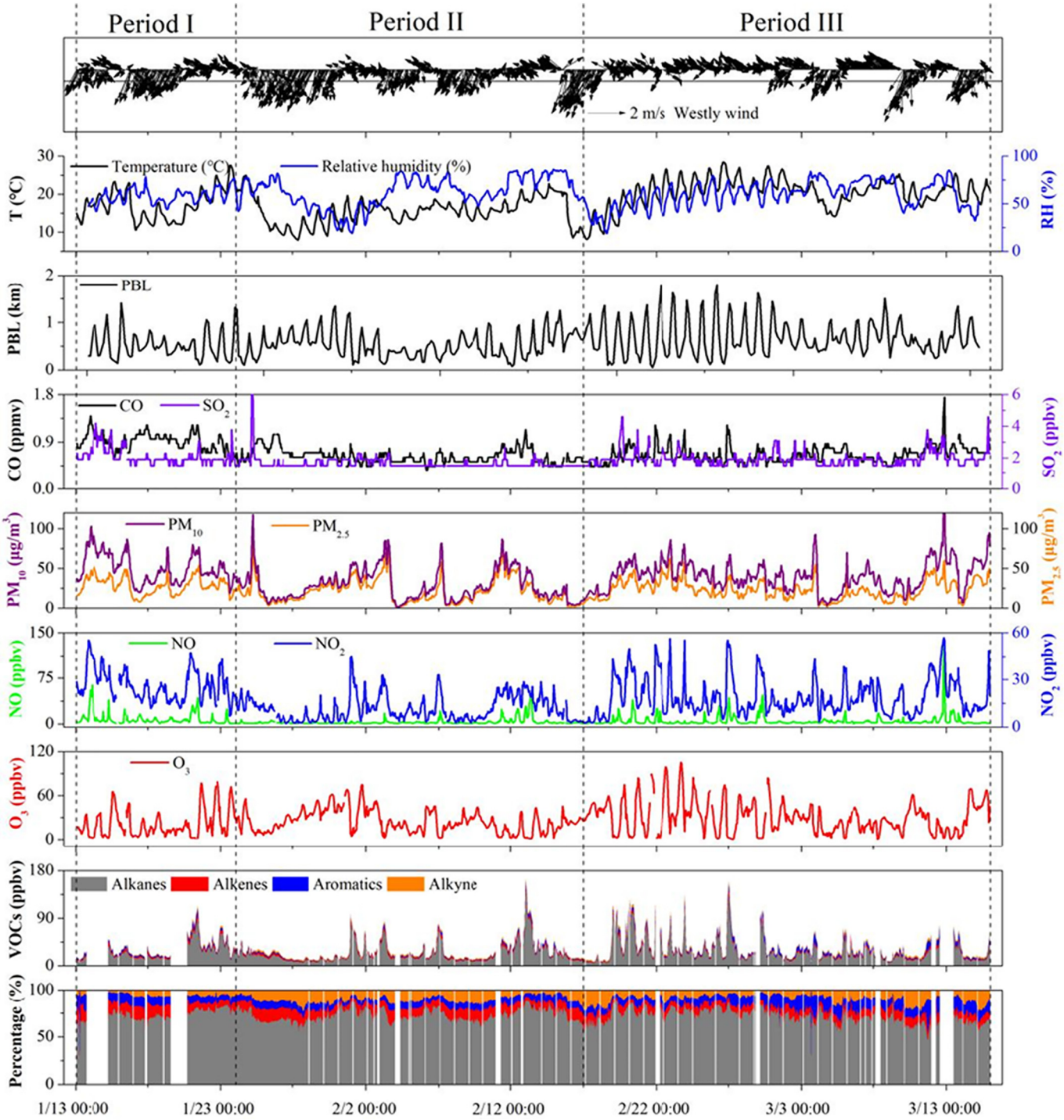

Fig. 2. Time series of observed VOCs, O_3, NO, NO_2, PM_{10}, $PM_{2.5}$, CO, SO_2 and meteorological parameters (planetary boundary layer, temperature, relative humidity, wind speed, wind direction) at GEMC in the three periods.

Table 1
Changing air quality and meteorological data observed at GEMC in the three periods.

	Period I		Period II		Period III	
	Range	Mean (95% C.I.)	Range	Mean (95% C.I.)	Range	Mean (95% C.I.)
T(° C)	10.6–27.6	18.6 (0.5)	8.0–25.0	16.2 (0.3)	8.1–28.4	21.3 (0.3)
RH (%)	42–78	58 (1)	19–86	59 (1)	19–85	64 (1)
WS (m/s)	0.3–2.6	1.1 (0.1)	0.3–3.5	1.2 (0.1)	0.2–3.9	1.1 (0.1)
PBL (m)	110–1409	511 (61)	77–1343	527 (39)	50–1780	676 (49)
CO (ppm)	0.52–1.40	0.91 (0.02)	0.35–1.05	0.63 (0.01)	0.44–1.75	0.67 (0.01)
SO_2 (ppb)	1.5–4.2	2.1 (0.1)	1.5–6.1	1.7 (0.0)	1.5–4.6	1.9 (0.0)
PM_{10} ($\mu g\ m^{-3}$)	19–103	50 (2)	1–118	28 (2)	3–146	40 (1)
$PM_{2.5}$($\mu g\ m^{-3}$)	8–54	28 (1)	1–86	21 (1)	2–63	23 (1)
NO (ppb)	0.8–63.6	7.8 (1.2)	0.8–44.9	2.9 (0.4)	0.0–133.7	5.0 (0.8)
NO_2 (ppb)	6.9–55.3	26.1 (1.2)	2.1–45.2	11.6 (0.6)	2.7–56.9	19.0 (0.9)
O_3–1h (ppb)	1.6–78.7	20.9 (2.2)	1.1–75	24.5 (1.3)	0.5–105.3	29.9 (1.7)
O_3-MDA8 (ppb)	12.2–64.4	38.3 (12.8)	11.2–65.4	34.0 (6.5)	13.3–87.8	49.5 (7.9)
Alkanes (ppb)	7.70–90.59	25.66 (2.35)	5.81–142.9	20.67 (1.50)	4.49–136.4	24.98 (1.66)
Alkenes (ppb)	0.95–11.77	3.43 (0.27)	0.48–8.42	2.58 (0.13)	0.14–12.31	2.57 (0.13)
Aromatics (ppb)	0.93–8.64	3.09 (0.22)	0.55–8.52	1.90 (0.11)	0.43–20.36	3.54 (0.23)
Alkynes (ppb)	0.45–5.20	1.85 (0.15)	0.59–6.23	2.36 (0.07)	0.61–10.71	2.71 (0.11)
VOCs (ppb)	11.66–112.1	34.01 (2.87)	9.65–162.5	27.51 (1.74)	7.52–158.3	33.79 (1.98)

42.9%, 9.5%, 72.4%, 63.8%, 6.3%, and 11.8%, respectively, due to the gradual recovery of socioeconomic and industrial activities. On average, the total VOCs before (34.01 ppb) and after (33.79 ppb) were quite close to each other, and they were approximately 23% higher than those during the lockdown (Table 1).

While ambient levels of $PM_{2.5}$ dropped in Period II due to decreased primary emissions and secondary formation from precursors such as SO_2, NOx and VOCs, ambient levels of O_3, an air pollutant secondarily formed from photochemical reaction of VOCs and NOx under sunlight, showed even higher average O_3–1h concentrations in Period II (24.5 ppb) than in Period I (20.9 ppb) (Table 1). Similar variations were also observed in Hangzhou, China, and in Rio de Janeiro, Brazil (Siciliano et al., 2020; Wang et al., 2020c). Compared to period I, a larger percentage drop of NOx (57.0%) than VOCs (19.1%) in period II would result in higher VOCs/NOx ratios (Fig. S1), leading to the weakened titration of O_3 by NO and thereby increasing average O_3 levels. However, as shown in Table 1, the daily maximum 8-h average O_3 (MDA8-O_3) did become slightly lower in Period II (34.0 ppb) than in Period I (38.3 ppb). As showed in Fig. 3, diurnal variations of O_3 in the three periods revealed the lowest afternoon O_3 levels during the lockdown, yet the average O_3–1h concentration during the lockdown (24.5 ppb) was higher than before (20.9 ppb) due to higher nighttime O_3 levels occurring with less NO titration during the lockdown. Ambient NO observed at the urban site GEMC during the lockdown decreased, particularly at night (Fig. 3), since the contribution from vehicular emissions, a dominant source of NO in urban areas, was reduced tremendously because of the lockdown.

3.2. Mixing ratios and compositions of VOCs

The ranges and means of the mixing ratios of speciated VOCs observed during the three periods are presented in Table S2. The total mixing ratios of VOCs ranged 11.66–112.1 ppbv with an average of 34.01 ± 2.87 ppbv in Period I and ranged 9.65–162.5 ppbv with an average 27.51 ± 1.74 ppbv in Period II with an average reduction rate of 19.1% when compared to that in Period I. In Period III, the total mixing ratio of VOCs on average recovered to be almost identical to that in Period I (Table S2; Fig. 4). Ozone formation potentials (OFPs) were further calculated based on localized maximum incremental reactivity (MIR) scales in Guangzhou city (Zhang et al., 2021). Consequently, the estimated OFPs decreased by 41.9% in Period II during the lockdown relative to Period I, and after the lockdown in Period III OFPs of VOCs became ~10% lower than that in Period I (Fig. 4). The SOA formation potentials (SOAFPs) under high-NOx and low-NOx conditions (Ng et al., 2007; Lim and Ziemann, 2009) were also calculated and results revealed that SOAFPs decreased by 44.7% in period II relative to period I under low-NOx conditions and by 51.4% under high-NOx conditions (Fig. 4). A larger decrease of SOAFPs from alkanes might be related to much larger decrease of high alkanes (C ≥ 6) than light alkanes (C < 6) as mentioned below. After the lockdown, the SOAFPs of VOCs in Period III recovered to only ~6% lower under low-NOx conditions and only 22.4% lower under high-NOx conditions when compared to those in Period I.

Alkanes were the most abundant VOC group in all three periods, with quite similar contribution percentages of 75.5%, 75.1% and 73.9% in the three periods. Alkenes accounted for 10.1% in Period I and 9.4% in Period II, higher than the 7.6% in Period III. The percentage of aromatics was the lowest in Period II (6.9%) when compared to that of 9.0% in Period I and 10.5% in Period III. While the less reactive alkanes decreased by 19.0% from Period I to Period II, the reactive alkenes and aromatics experienced larger decreases of 24.8% and 38.3%, respectively (Fig. 4). Since aromatics were widely used as industrial solvents in the study area (Zheng et al., 2013), a larger decrease in ambient aromatics in Period II reflects a significant reduction in industrial emissions due to the province-wide shutdown of the majority of factories, similar to those during the 2014 Asian-Pacific Economic Cooperation summit in Beijing (Li et al., 2015; Yang et al., 2018) and the 2016 G20 summit in Hangzhou (Zhang et al., 2020) with enhanced control of industrial emissions. After the lockdown in Period III, while enterprises gradually resumed production, reactive aromatics increased by 86.4%, alkanes only increased by 20.6%, and alkenes, however, almost did not change on average when compared to those in Period II. In addition, it is worth noting that on average alkanes decreased by 19.0% in Period II relative to Period I, light alkanes (C < 6), which are related to liquefied petroleum gas (LPG) and gasoline evaporation emissions, decreased by only 13.0% while higher alkanes (C ≥ 6), which are largely related to vehicle exhaust and industrial solvents, decreased by 67.8%, further confirming larger VOC emission reductions in industry and transportation sectors during the lockdown. As for the OFPs of different VOC groups, aromatics attributed the most to OFPs in all three periods, with a share of 40.4%, 38.5% and 51.2% of OFPs before, during and after the COVID-19 lockdown, respectively. Alkanes contributed 30.7%, 30.3% and 28.0% of OFPs, while alkenes contributed 28.8%, 30.2% and 20.2% of OFPs before, during and after the COVID-19 lockdown.

Changes in mixing ratios for major VOC species during the lockdown are shown in Fig. 5. Among the most abundant alkanes, propane, n-butane, i-butane, and i-pentane decreased by 13–29% in Period II relative to those in Period I, and ethane instead increased by 15.7% on average (Fig. 5a; Table S2). This increase in ethane probably reflects more indoor activities (such as cooking) during the lockdown with more LNG-related emissions of ethane in the densely populated urban areas, since LNG (over 95% methane along with a few percent ethane) is predominantly used for cooking and in LNG-fired small boilers for bathing in Guangzhou, and its leakage and incomplete combustion would lead to emissions of ethane (Speight, 2015). Reactive alkenes and aromatics all decreased during the lockdown (Fig. 5b; Table S2). Among the three most abundant alkenes,

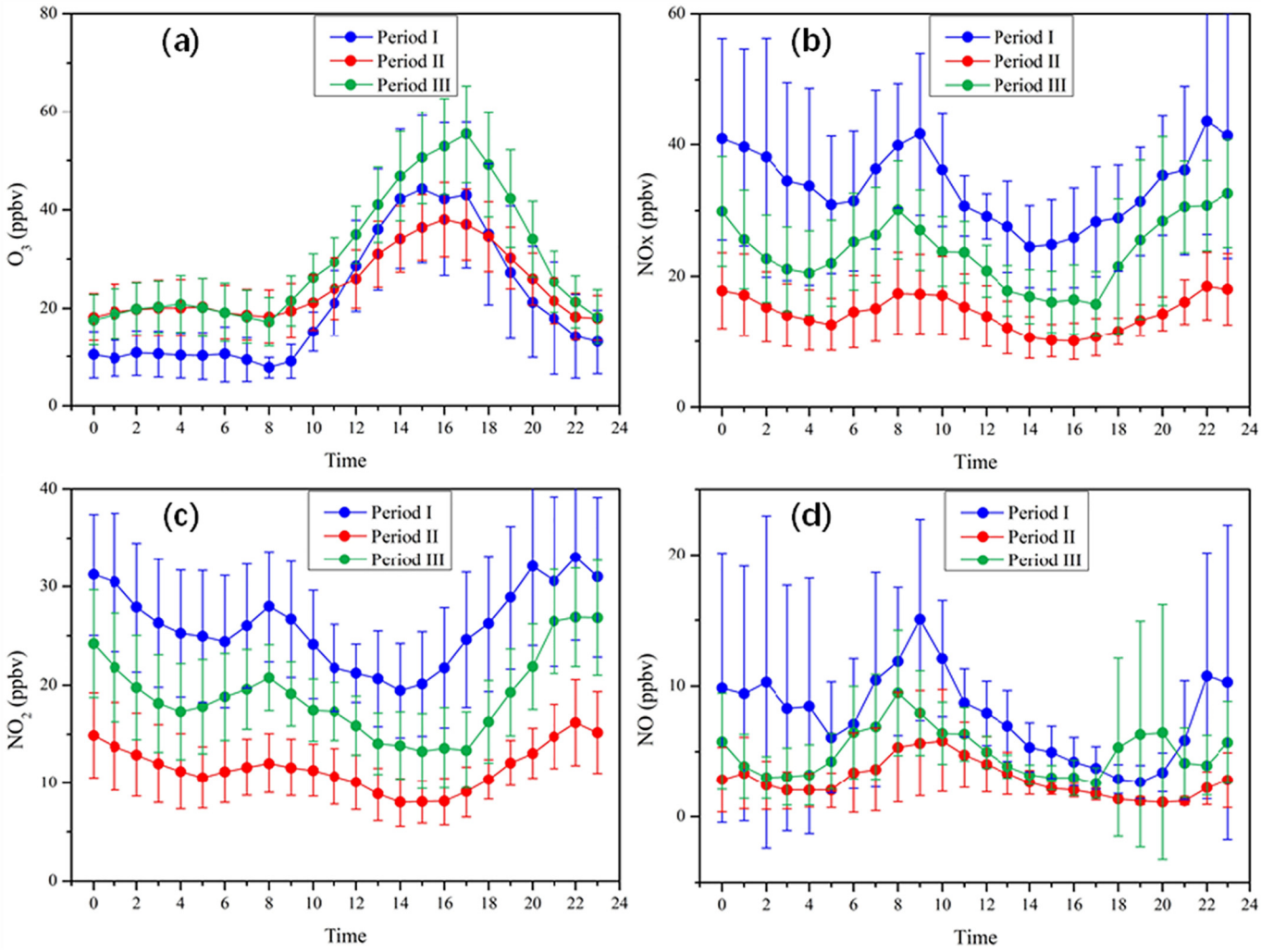

Fig. 3. Diurnal variations in (a) O_3, (b) NOx, (c) NO_2 and (d) NO at GEMC in the three periods.

1-butene decreased by 55.1% and propene by 25.8%, while ethene dropped very slightly on average, probably also due to enhanced residential LNG/LPG combustion-related emissions. Toluene, ethylbenzene, and xylenes decreased by over 40% in Period II compared with Period I, while benzene only dropped by nearly 10% on average (Fig. 5b; Table S2). This might result from the fact that benzene is forbidden to use in industry, while other aromatics are widely used industrial solvents or feedstocks (Liu et al., 2017; Zhang et al., 2015; Zheng et al., 2013).

3.3. Temporal variations of VOCs

The time series of total and grouped VOCs are shown in Fig. 2. A VOC pollution episode was observed on January 21st in Period I with the mixing ratio of VOCs reaching as high as 112.1 ppbv in the morning, while in Period II, VOC pollution episodes occurred on January 31st, February 3rd, and during February 6-7th and February 11-13th. During the February 11-13th episode, the mixing ratio of VOCs increased from 27.65 ppbv at 0:00 on February 11th to 162.5 ppbv at 0:00 on February 13th. The higher mixing ratios of VOCs appeared to be accompanied by low wind speeds (Fig. 2), suggesting their accumulation under unfavorable dispersion conditions. Meanwhile, wind direction also seemed to impact the increase in VOC concentrations during the episodes. During the February 11-13th episode, for example, mixing ratios of VOCs were lower than 20 ppbv before February 10th when northerly wind prevailed; however, they increased to 42 ppbv on February 11th and to 54 ppbv on February 12th as the wind speed gradually decreased and its direction turned southerly. It is worth noting that although the average concentrations of air pollutants dropped substantially in Period II due to the COVID-19 lockdown, four pollution episodes still occurred with increased concentrations of VOCs, NO_2 and $PM_{2.5}$ under unfavorable weather conditions. This indicates that emission reductions as strong as that induced passively by the COVID-19 lockdown could not completely eliminate the occurrence of air pollution. After the lockdown, the concentrations of VOCs, NO_2, $PM_{2.5}$, and SO_2 all increased from February 19th, and the mixing ratio of O_3 also increased gradually with hourly maxima of 72 ppbv on the 19th and 101 ppbv on the 23rd.

For the diurnal variations shown in Fig. 6, one distinction is that an obvious peak for total VOCs and alkanes was observed in the morning rush hours due to the influence of vehicular emissions in Period I and Period III (Baudic et al., 2016; Liu et al., 2016), but this peak disappeared in Period II (Fig. 6) because of much less traffic with the strict quarantine, as also reflected by the all-day lower NOx levels in Period II (Fig. 3). Another distinction is that reactive alkenes and aromatics had significantly lower concentrations than those in Period I throughout the day, with wider gaps than total VOCs and alkanes between the two periods, suggesting that reactive alkenes and aromatics were reduced at a comparatively larger scale during the lockdown, particularly for aromatics (Fig. 6). It should be noted that while alkanes and aromatics recovered in Period III after the lockdown to levels that were comparable to those in Period I before the lockdown, alkenes in Period III remained at levels similar to those in Period II, implying that emissions of alkenes were much less impacted than those of aromatics by increased industry activities and traffic in Period III.

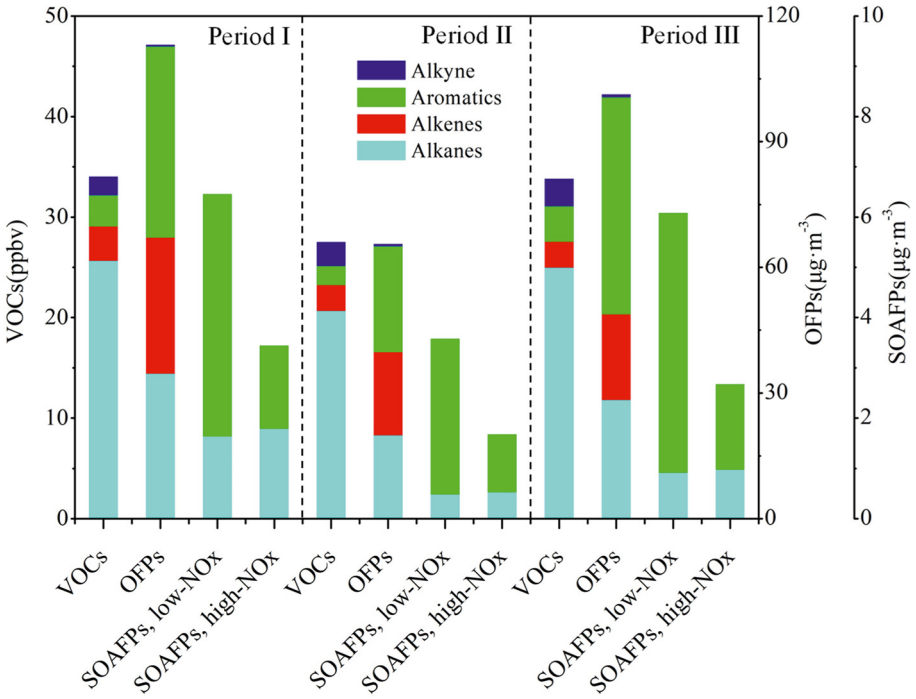

Fig. 4. Mixing ratios and chemical compositions of VOCs, as well as their ozone formation potentials (OFPs) and SOA formation potentials (SOAFPs), at GEMC in the three periods.

Toluene and benzene can be present in combustion emissions such as coal burning emissions, vehicle exhaust and biomass burning (Moreira dos Santos et al., 2004; Zhang et al., 2012), and solvent use is among the most important sources of toluene, while benzene is prohibited in industrial solvents (Wang et al., 2014; Yuan et al., 2010). Previous studies revealed a T/B ratio of <1 for biomass/biofuel/coal burning emissions (Liu et al., 2015; Moreira dos Santos et al., 2004), ~1.6 for vehicle exhaust emissions (Wang et al., 2002b; Li et al., 2020c), and much higher for industrial solvent use (Chan et al., 2006). The average T/B ratios were 1.83 ± 0.16, 1.20 ± 0.11, and 3.45 ± 0.18 in Periods I, II, and III, respectively, also implying reduced industrial solvent use and vehicle emissions of aromatics during the lockdown.

The differences in T/B ratios could be further investigated from the diurnal variations (Fig. 7). In Periods I and III, slightly increased T/B ratios during morning rush hours reflected the influence of vehicle emission. An

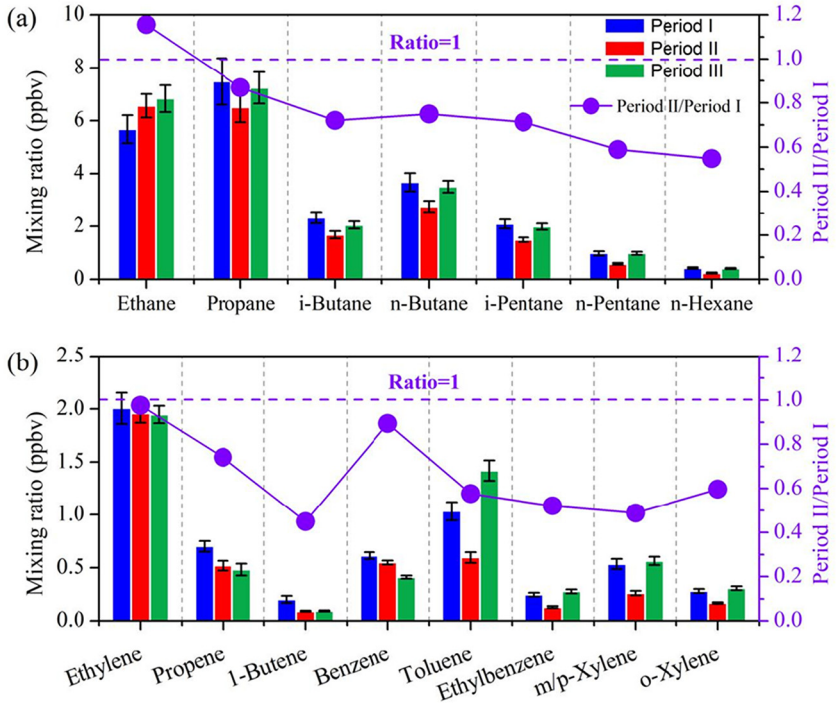

Fig. 5. Comparison of typical VOCs in the three periods. The circles indicate the ratios of Period II/Period I for typical VOCs. The error bar indicates the 95% confidence interval (95% C.I.).

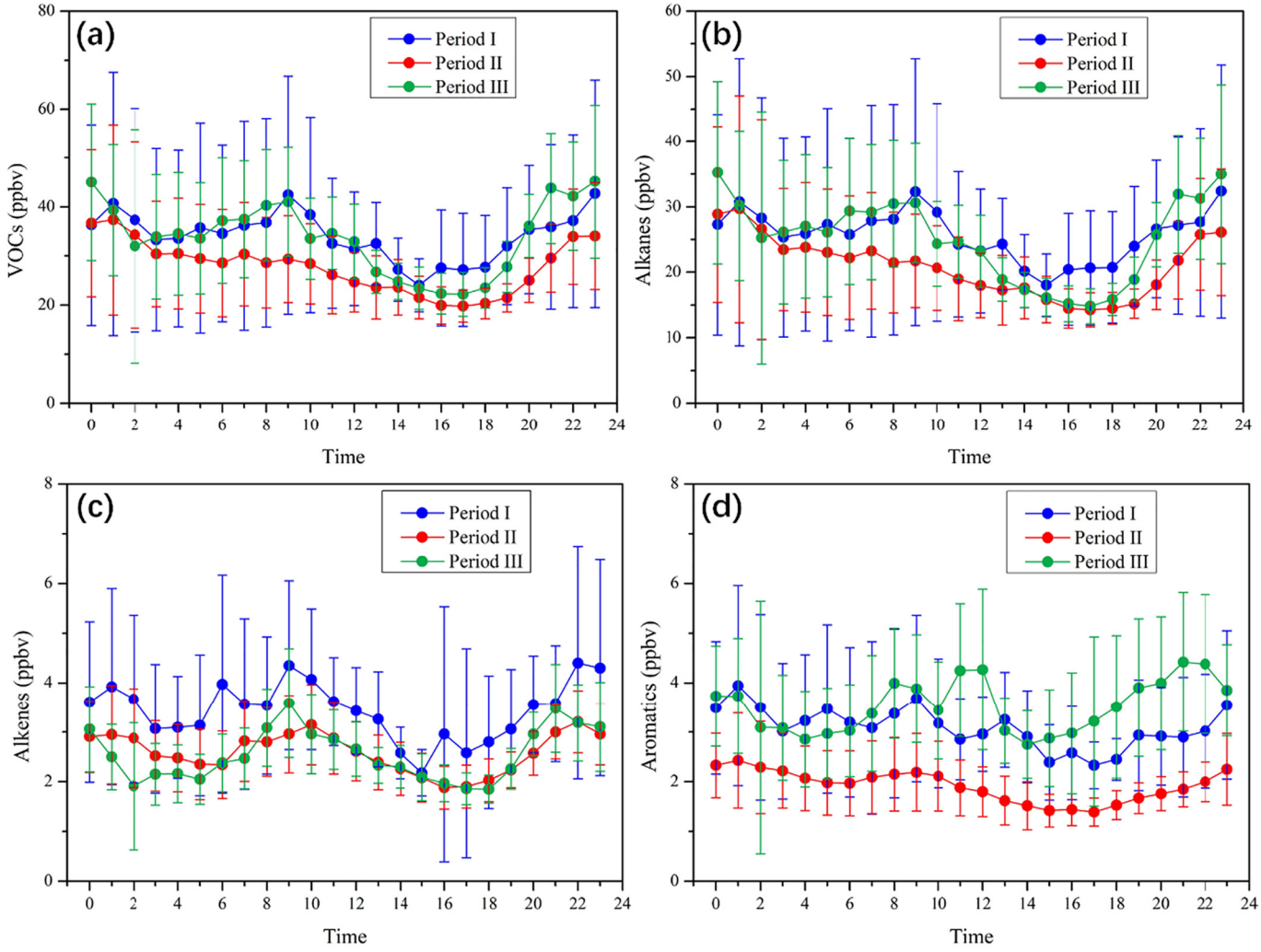

Fig. 6. Diurnal variations of (a) VOCs, (b) alkanes, (c) alkenes and (d) aromatics at GEMC in the three periods.

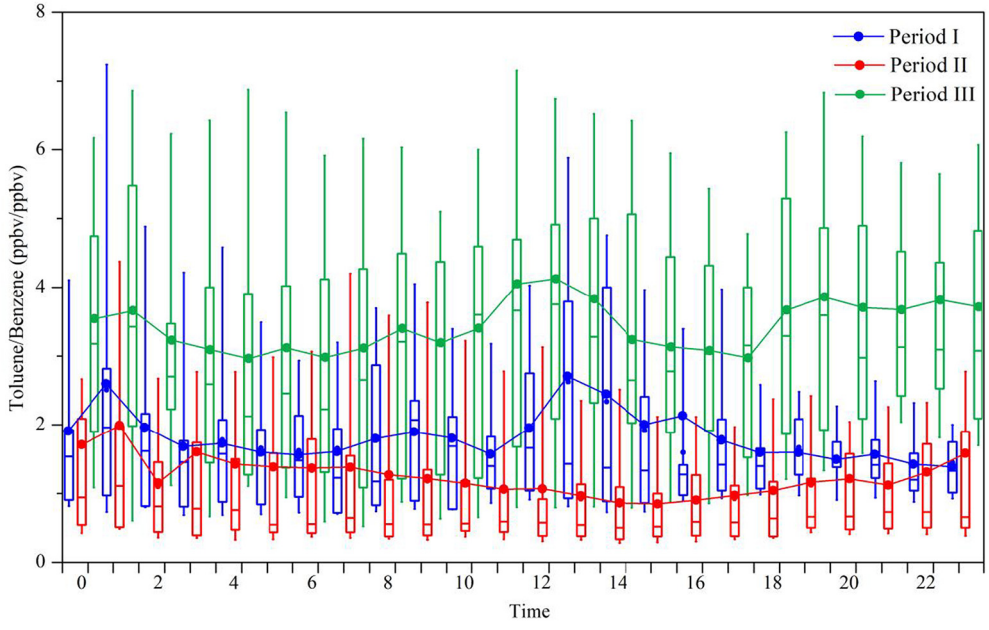

Fig. 7. Diurnal variations in the toluene to benzene ratio (T/B) in the three periods. The lower and upper boundaries of the box represent the 25th and 75th percentiles, respectively; the whiskers below and above the box indicate the 10th and 90th percentiles, respectively; the line within the box marks the median; and the dot represents the mean.

obvious peak of T/B ratios appeared in the afternoon (12:00–16:00). This peak could not be explained by higher oxidation rates of toluene relative to benzene, but by elevated evaporation of solvents at higher temperatures. As toluene is a widely used solvent in industry, its enhanced evaporation would give rise to T/B ratios. In Period II, however, no T/B peak was found at morning rush hours or in the afternoon, and T/B decreased continuously from 03:00 to 15:00 and then began to increase until 01:00 of the next day due to the influence of photochemical oxidation and changing mixing layer heights (Liu et al., 2020).

3.4. Source apportionment with PMF

3.4.1. Source identification

To further quantify the contributions by different sources to ambient VOCs at three periods, the 28 most important species were selected for source apportioning with the PMF receptor model. The PMF was run with factor numbers increasing from 3 to 7. As showed in Fig. S2a, Q/Q_{exp} values decreased gradually with the factor number, and the decrease rates turned lower when factor number was 6 or higher. Meanwhile, a new source was extracted when factor number increased from 3 to 5 (Fig. S2b). As factor number reached 6 or higher, two factors would refer to one emission sources and it was hard to represent real-world emissions. Therefore, the five-factor solution was chosen in this study, and the PMF reconstructed masses matched the measured ones very well, with a slope (reconstructed to measured) of 0.95 and r^2 of 0.99 (Fig. S2c).

The profiles of five sources resolved by PMF are showed in Fig. S3. Factor 1, with high loadings of ethylene (41.6%), ethyne (27.5), 3-methylhexane (53.6%), toluene (26.6%) and benzene (18.5%), is typical of gasoline vehicle emissions with a T/B near 1.5 (Watson et al., 2001; Wu et al., 2016; Yang et al., 2018; Zhang et al., 2013) and therefore is regarded as gasoline-related emissions (gasoline vehicle exhaust and gasoline evaporation). Factor 2 was dominated by methylcyclopentane, n-decane, 1,2,4-trimethylbenzene and 1,2,3-trimethylbenzene, which are typical tracers in exhaust from diesel-powered engines (Song et al., 2007; Zhang et al., 2012, 2018; Wu et al., 2020) and thus can be identified as diesel exhaust (including diesel vehicle exhaust and non-road diesel engines). Factor 3 was rich in ethane, propane, i-butane, n-butane, propene and 1-butene. Propane, i-butane, and n-butane are the main components of LPG, which are widely used in cooking and as fuel for taxis and buses (Zhang et al., 2018; McCarthy et al., 2013). Previous studies also indicated that ethane, propene and butenes were also associated with LPG-fueled vehicle exhaust (Tang et al., 2008; Feng et al., 2020). Therefore, this factor is attributed to LPG related sources. Factor 4 was distinguished by high percentages of ethylene, ethyne, benzene, CO and C_4-C_5 species. Ethylene and ethyne are important species emitted from biomass open burning (Fang et al., 2017). C_4-C_5 VOCs and benzene are also the main components in emissions from coal burning (Hui et al., 2019; Liu et al., 2008; Wu et al., 2016). Thus, this factor is related to biomass/coal burning. Factor 5 was rich in toluene, ethylbenzene, xylenes and styrene. Solvent use and vehicle exhaust were important sources of aromatics (Ou et al., 2015; Zhang et al., 2012), while poor correlation between aromatics and combustion tracers in factor

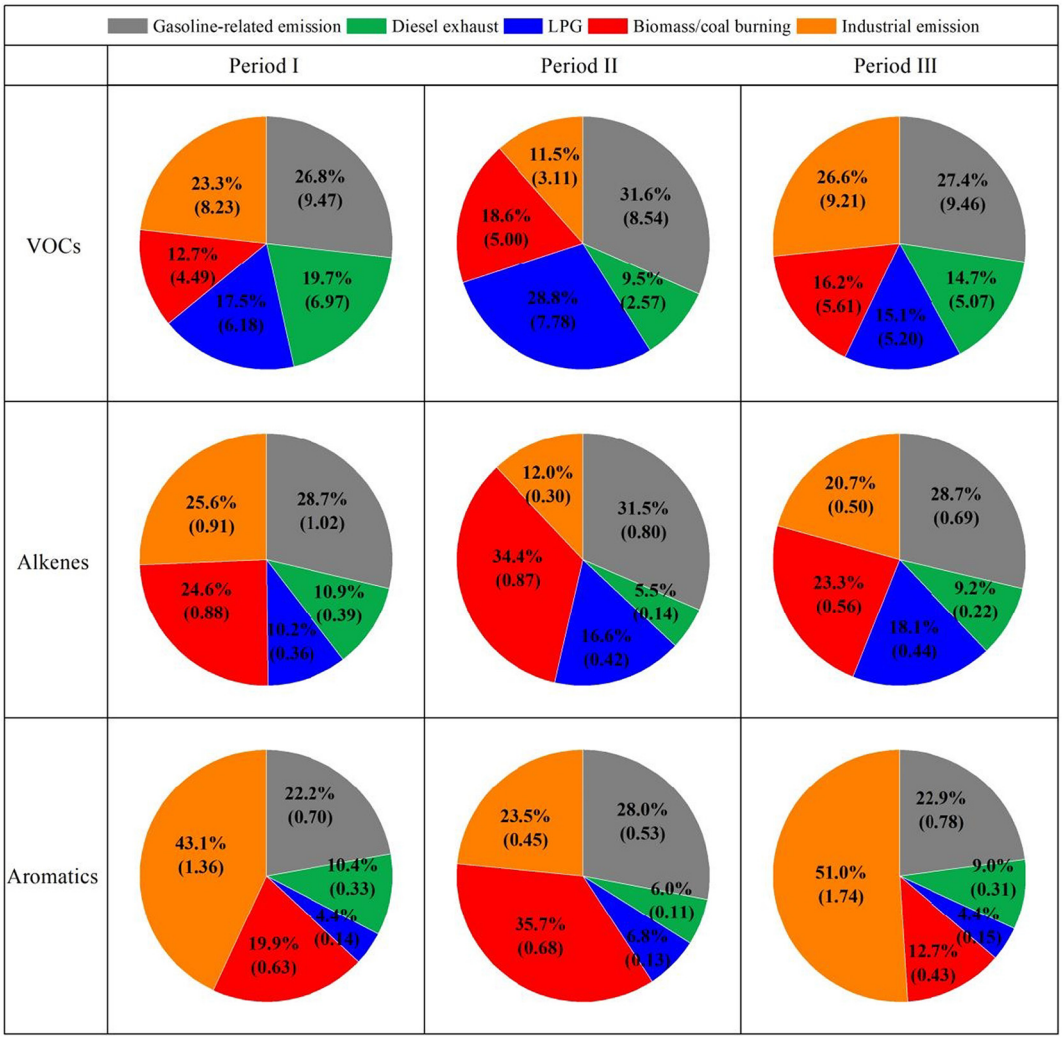

Fig. 8. Source contributions to VOCs, alkenes, and aromatics in three periods at GEMC.

5 (such as ethyne and CO) indicated that the above species in this factor were largely associated with solvent use. n-Octane can be used as a solvent in paint and liquid process photocopiers (Shao et al., 2016). 2,3,4-Trimethylpentane is widely used in solvents for household and consumer production industries (Guo et al., 2011). Therefore, higher n-octane and 2,3,4-trimethylpentane also confirm that this factor can be assigned to industrial emissions.

3.4.2. Changing VOCs source contributions

As shown in Fig. 8, gasoline-related emission was the largest source during the three periods, accounting for 26.8%, 31.6%, and 27.4% of VOCs, respectively. The contribution percentages of industrial emission and diesel exhaust decreased from 23.3% and 19.7% in Period I to 11.5% and 9.5% in Period II, respectively. Instead, the contributions of biomass/coal burning and LPG increased from 12.7% and 17.5% in Period I to 18.6% and 28.8% in Period II, respectively. As shown in Fig. 9, for the time series of source contributions, industrial emissions deceased the most from January 13th to January 31st among the five sources, consistent with larger declines in the level of aromatics and in ratios of toluene or xylenes to CO. In Period III, with the gradual easing of pandemic lockdown measures, the contribution percentages of industrial emission and diesel exhaust returned to 26.6% and 14.7%, while those of LPG and biomass burning shrank again to 15.1% and 16.2%, respectively.

When compared to that in Period I, the contribution from industrial emissions on average was reduced more than that from other sources in Period II, accounting for 48.9% of the reduction in ambient VOCs during the lockdown (Fig. 9). Meanwhile, emission reductions from diesel exhaust and gasoline-related emission could explain 42.2% and 8.9% of the total VOC

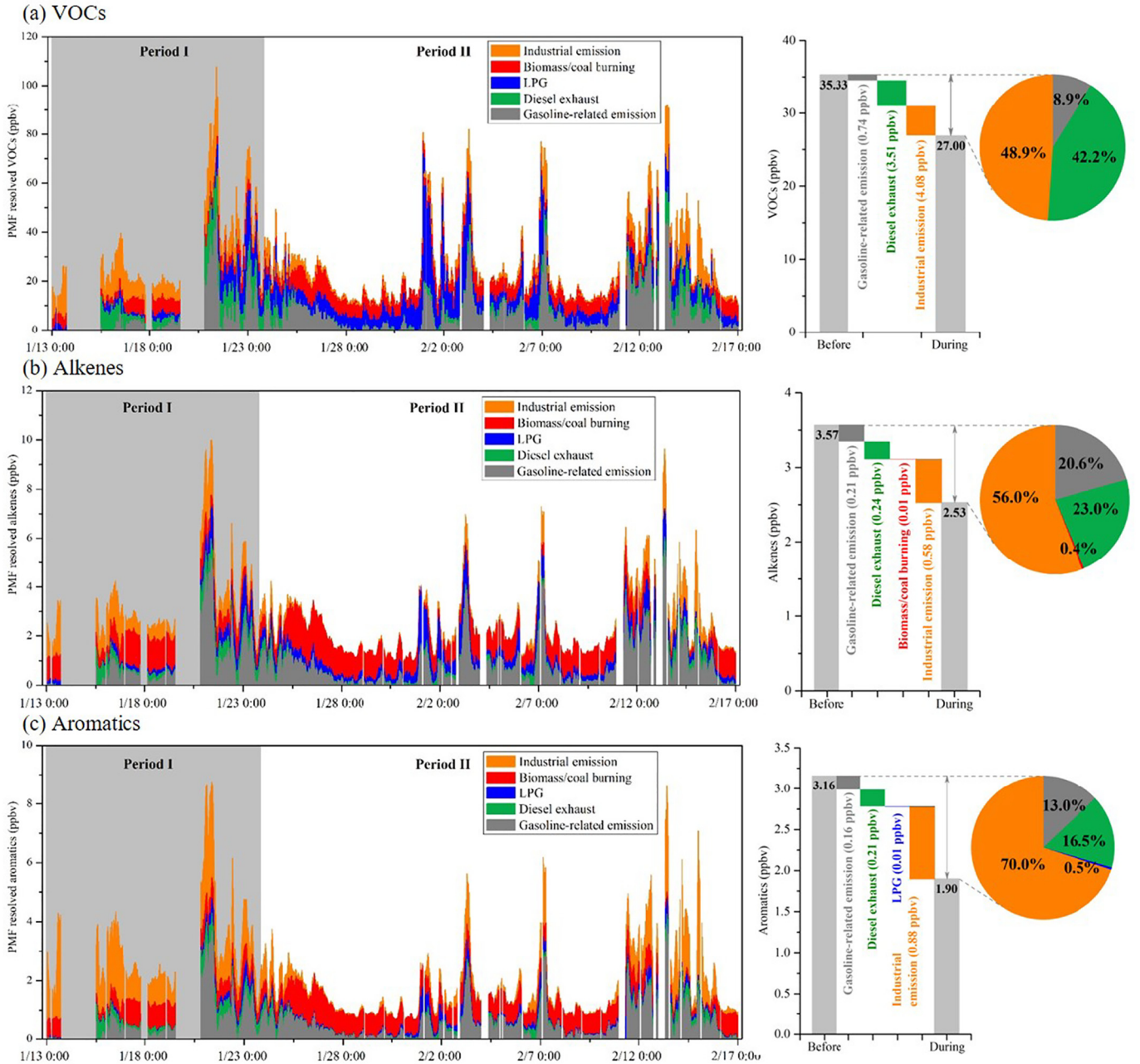

Fig. 9. Time series of PMF resolved contribution and decomposed changes by emission sources for mixing ratio of (a) VOCs, (b) alkenes and (c) aromatics during the campaign. On the right the bars show decreased ambient levels explained by source emission reductions during the lockdown, and pies indicate the percentages of decreased ambient levels due to reductions of different source emissions.

reduction. Diesel exhaust emissions decreased much more than gasoline-related emissions in Period II, probably because on-road vehicles are mostly gasoline-powered private cars during this period (Qi et al., 2021) and because the use of diesel-powered trucks and non-road engines (such as construction machines) was reduced tremendously with almost frozen industry activities. Biomass/coal burning revealed a higher contribution percentage in Period II because of decreased contributions from traffic and industry. In contrast, LPG-related emissions had a burden increasing from 6.18 ppbv in Period I to 7.78 ppbv in Period II. This might be related to much more use of LPG as a result of increased indoor activities.

The contributions of OFPs by different emission sources could be further calculated based on the PMF results. As showed in Fig. 10, gasoline-related emission, industrial emission, and biomass/coal burning were the three most important sources of OFPs, attributing 31.6%, 28.9%, and 17.2% of OFPs, before the COVID-19 lockdown, respectively. During the lockdown, the contribution percentages of industrial emission and diesel exhaust decreased to 19.1% and 5.5%, respectively, while those of biomass/coal burning and LPG increased to 23.5% and 18.0%. In period III, industrial emission increased significantly and contributed the most (35.1%), followed by gasoline-related emission (27.1%) and biomass/coal burning (19.9%), while the contribution of diesel exhaust increased to 8.1% with more use of diesel-powered trucks and non-road engines.

3.4.3. Source contributions to reactive alkenes and aromatics

As mentioned above, reactive alkenes and aromatics decreased more significantly during the COVID-19 lockdown. As shown in Fig. 8, the contribution of gasoline-related emission, biomass/coal burning, and LPG to alkenes increased from 28.7%, 24.6%, and 10.2% in Period I to 31.5%, 34.4%, and 16.6% in Period II. In contrast, industrial emission and diesel exhaust contributed less alkenes in Period II (12.0% and 5.5%) than in Period I (25.6% and 10.9%), respectively. Since the COVID-19 lockdown, the PMF-resolved diesel vehicle exhaust and industrial emission gradually decreased (Fig. 9), and the changes in industrial emission, diesel exhaust, and gasoline-related emissions could explain 56.0%, 23.0%, and 20.6% of the reduction in reactive alkenes, respectively.

Industrial emission, gasoline exhaust and biomass/coal burning were the three most important sources of aromatics in Period I, with contributions of 43.1%, 22.2% and 19.9%, respectively (Fig. 8). In Period II, however, biomass/coal burning contributed the most to aromatics (35.7%), followed by gasoline-related emission (28.0%) and industrial emission (23.5%). It is worth noting that reductions in industrial emission, diesel exhaust and gasoline-related emission could explain 70.0%, 16.5% and 13.0% of the total reduction of aromatics in Period II relative to Period I (Fig. 9), respectively. In Period III, aromatics from industrial emission increased rapidly with a contribution percentage of 51.1%, consistent with the much greater increase in the levels of aromatics after the lockdown.

4. Conclusions

The unusual passive emission reductions during the COVID-19 lockdown offered an opportunity to look into the impacts of changing anthropogenic emissions (particularly in the heavily-affected industry and transportation sectors) on ambient levels of reactive VOCs. During the lockdown, PM_{10}, $PM_{2.5}$, CO and SO_2 dropped by 44%, 25%, 32% and 21%, respectively, while average O_3–1h concentrations increased by 17% but average MDA8-O_3 decreased by 11% when compared to those before the lockdown. These changes in O_3 were achieved when O_3 precursors NOx and VOCs decreased by 57.0% and 19.1%, respectively. At urban sites where O_3 formation is typically VOC-limited, solely reducing NOx emissions might induce elevated O_3 levels. The results from this study demonstrate that reduction in ambient NOx levels as high as 57% would result in less significant changes in ambient O_3 levels, or even lower MDA8-O_3, if ambient levels of VOCs, particularly those of more reactive aromatic and alkene species, were reduced at the same time.

While average mixing ratios of VOCs became 19.1% lower during the lockdown than before, mixing ratios of reactive alkenes and aromatics decreased by 24.8% and 38.2%, respectively, and alkanes decreased by 19.0%. Specifically, on average mixing ratios of light alkanes ($C < 6$) decreased by only 13.0% while those of higher alkanes ($C \geq 6$) decreased by 67.8% during the lockdown. Based on results from the PMF receptor model, decreased ambient VOC levels during the lockdown could be largely attributed to reduced industrial emissions, diesel exhaust and gasoline-related emissions, which could account for 48.9%, 42.2% and 8.8% of reductions in ambient VOCs, respectively. Moreover, the reduction in industrial emissions could explain 56.0% and 70.0% of the reduction in ambient reactive alkenes and aromatics, respectively. It is worth noting that reduction in diesel exhaust emissions contributed substantially to the reduction in ambient levels of VOC, particularly those of heavier alkanes. This might be not only resulted from reduction in on-road diesel vehicle emissions, but also from reduction in emissions from non-road diesel engines (like construction machines), which were much loosely controlled in exhaust emissions and yet were much more heavily impacted by the lockdown.

CRediT authorship contribution statement

C.L.P.: Data curation, Writing original draft; W.Q.Y.: Writing, Methodology; Y.L.Z.: Conceptualization, Writing, Methodology; W.S., S.X.X., J.W., J.P.Z: Software, Investigation, Methodology; D.H.C., Y.J.W., Y.N.C.: Investi-

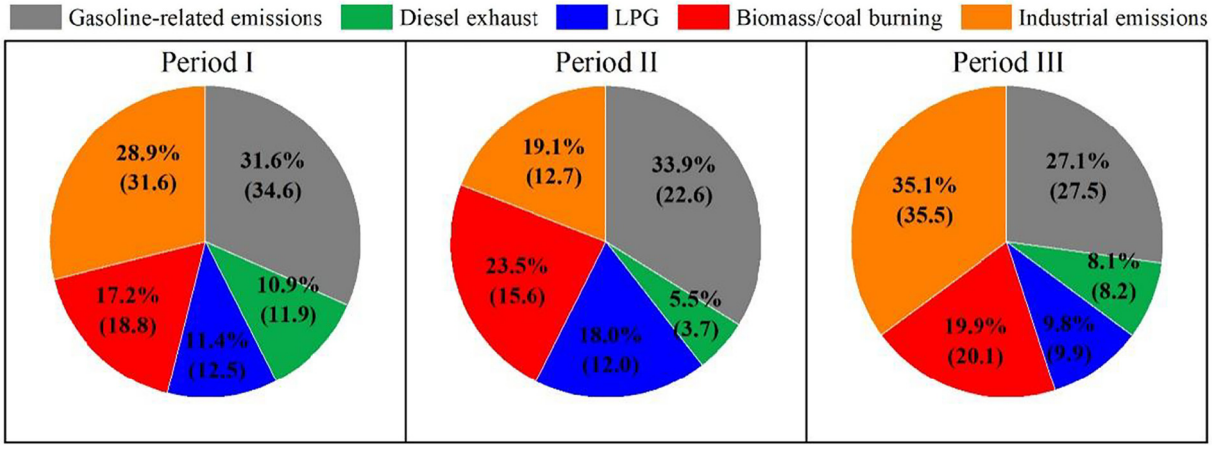

Fig. 10. Source contributions of OFPs in the three periods at GEMC.

gation, Formal analysis; X.M.W.: Conceptualization, Supervision, Project administration, Writing – review & editing.

Declaration of competing interest

The authors declare that they have no known competing financial interests or personal relationships that could have appeared to influence the work reported in this paper.

Acknowledgments

This study was supported by the National Natural Science Foundation of China (Grant No. 41961144029), the Chinese Academy of Sciences (Grant No. QYZDJ-SSW-DQC032/XDA23010303/XDA23020301/XDPB1901), the Hong Kong Research Grant Council (T24-504/17-N), and Department of Science and Technology of Guangdong Province (2020B1212060053/2017BT01Z134/2019B121205006).

Appendix A. Supplementary data

Supplementary data to this article can be found online at https://doi.org/10.1016/j.scitotenv.2022.153720.

References

Atkinson, R., 2000. Atmospheric chemistry of VOCs and NOx. Atmos. Environ. 34, 2063–2101. https://doi.org/10.1016/S1352-2310(99)00460-4.

Baudic, A., Gros, V., Sauvage, S., Locoge, N., Sanchez, O., Sarda-Estève, R., Kalogridis, C., Petit, J.E., Bonnaire, N., Baisnée, D., 2016. Seasonal variability and source apportionment of volatile organic compounds (VOCs) in the Paris megacity (France). Atmos. Chem. Phys. 16, 11961–11989. https://doi.org/10.5194/acp-16-11961-2016.

Bian, Y., Huang, Z., Ou, J., Zhong, Z., Xu, Y., Zhang, Z., Xiao, X., Ye, X., Wu, Y., Yin, X., Li, C., Chen, L., Shao, M., Zheng, J., 2019. Evolution of anthropogenic air pollutant emissions in Guangdong Province, China, from 2006 to 2015. Atmos. Chem. Phys. 19, 11701–11719. https://doi.org/10.5194/acp-19-11701-2019.

Cai, S., Li, Q., Wang, S., Chen, J., Ding, D., Zhao, B., Yang, D., Hao, J., 2018. Pollutant emissions from residential combustion and reduction strategies estimated via a village-based emission inventory in Beijing. Environ. Pollut. 238, 230–237. https://doi.org/10.1016/j.envpol.2018.03.036.

Chameides, W.L., Fehsenfeld, F., Rodgers, M.O., Cardelino, C., Martinez, J., Parrish, D., Lonneman, W., Lawson, D.R., Rasmussen, R.A., Zimmerman, P., Greenberg, J., Middleton, P., Wang, T., 1992. Ozone precursor relationships in the ambient atmosphere. J. Geophys. Res.-Atmos. 97, 6037–6055. https://doi.org/10.1029/91JD03014.

Chan, L.Y., Chu, K.W., Zou, S.C., Chan, C.Y., Wang, X.M., Barletta, B., Blake, D.R., Guo, H., Tsai, W.Y., 2006. Characteristics of nonmethane hydrocarbons (NMHCs) in industrial, industrial-urban, and industrial-suburban atmospheres of the Pearl River Delta (PRD) region of South China. J. Geophys. Res.-Atmos. 111 (D11), D11304. https://doi.org/10.1029/2005JD006481.

Chang, S.C., Lin, T.H., Lee, C.T., 2009. On-road emission factors from light-duty vehicles measured in hsuehshan tunnel (12.9 km), the longest tunnel in Asia. Environ. Monit. Assess. 153, 187–200. https://doi.org/10.1007/s10661-008-0348-9.

Chen, K., Wang, M., Huang, C., Kinney, P.L., Paul, A.T., 2020a. Air Pollution reduction and mortality benefit during the COVID-19 outbreak in China. The Lancet Planetary Health 4 (6), E210–E212. https://doi.org/10.1016/S2542-5196(20)30107-8 2020b.

Chen, H., Huo, J., Fu, Q., Duan, Y., Xiao, H., Chen, J., 2020b. Impact of quarantine measures on chemical compositions of PM2.5 during the COVID-19 epidemic in Shanghai, China. Science of the Total Environment 743, 140758. https://doi.org/10.1016/j.scitotenv.2020.140758.

Chu, B., Zhang, S., Liu, J., Ma, Q., He, H., 2021. Significant concurrent decrease in PM2.5 and NO2 concentrations in China during COVID-19 epidemic. J. Environ. Sci. 99, 346–353. https://doi.org/10.1016/j.jes.2020.06.031.

Cui, Y., Ji, D., Maenhaut, W., Gao, W., Zhang, R., Wang, Y., 2020. Levels and sources of hourly PM2.5-related elements during the control period of the COVID-19 pandemic at a rural site between Beijing and Tianjin. Sci. Total Environ. 744, 140840. https://doi.org/10.1016/j.scitotenv.2020.140840.

Ding, A.J., Fu, C.B., Yang, X.Q., Sun, J.N., Zheng, L.F., Xie, Y.N., Herrmann, E., Nie, W., Petaja, T., Kerminen, V.M., Kulmala, M., 2013. Ozone and fine particle in the western Yangtze River Delta: an overview of 1 yr data at the SORPES station. Atmos. Chem. Phys. 13, 5813–5830. https://doi.org/10.5194/acp-13-5813-2013.

Doumbia, T., Granier, C., Elguindi, N., Bouarar, I., Darras, S., Brasseur, G., Gaubert, B., Liu, Y.M., Shi, X.Q., Stavrakou, T., Tilmes, S., Lacey, F., Deroubaix, A., Wang, T., 2021. Changes in global air pollutant emissions during the COVID-19 pandemic: a dataset for atmospheric modeling. Earth Syst. Sci. Data 13, 4191–4206. https://doi.org/10.5194/essd-2020-348.

Fang, Z., Deng, W., Zhang, Y.L., Ding, X., Tang, M.J., Liu, T.Y., Hu, Q.H., Zhu, M., Wang, Z.Y., Yang, W.Q., Huang, Z.H., Song, W., Bi, X.H., Chen, J.M., Sun, Y., George, C., Wang, X.M., 2017. Open burning of rice, corn and wheat straws: primary emissions, photochemical aging, and secondary organic aerosol formation. Atmos. Chem. Phys. 17 (24), 14821–14839. https://doi.org/10.5194/acp-17-14821-2017.

Feng, J., Zhang, Y., Song, W., Deng, W., Zhu, M., Fang, Z., Ye, Y., Fang, H., Wu, Z., Lowther, S., Jones, K.C., Wang, X., 2020. Emissions of nitrogen oxides and volatile organic compounds from liquefied petroleum gas-fueled taxis under idle and cruising modes. Environ. Pollut. 267, 115623. https://doi.org/10.1016/j.envpol.2020.115623.

Forstner, H.J.L., Flagan, R.C., Seinfeld, J.H., 1997. Secondary organic aerosol from the photooxidation of aromatic hydrocarbons: molecular composition. Environ. Sci. Technol. 31, 1345–1358. https://doi.org/10.1021/es9605376.

Guevara, M., Jorba, O., Soret, A., Petetin, H., Bowdalo, D., Serradell, K., Tena, C., Denier Van Der Gon, H., Kuenen, J., Peuch, V.H., Pérez García-Pando, C., 2021. Time-resolved emission reductions for atmospheric chemistry modelling in Europe during the COVID-19 lockdowns. Atmos Chem Phys 21, 773–797. https://doi.org/10.5194/acp-21-773-2021.

Guo, H., Cheng, H.R., Ling, Z.H., Louie, P.K.K., Ayoko, G.A., 2011. Which emission sources are responsible for the volatile organic compounds in the atmosphere of Pearl River Delta? J. Hazard. Mater. 188 (1–3), 116–124. https://doi.org/10.1016/j.jhazmat.2011.01.081.

Guo, S., Hu, M., Zamora, M.L., Peng, J., Shang, D., Zheng, J., Du, Z., Wu, Z., Shao, M., Zeng, L., Molina, M.J., Zhang, R., 2014. Elucidating severe urban haze formation in China. Proc. Natl. Acad. Sci. U. S. A. 111, 17373–17378. https://doi.org/10.1073/pnas.1419604111.

Huang, R.J., Zhang, Y.L., Bozzetti, C., Ho, K.F., Cao, J.J., Han, Y.M., Daellenbach, K.R., Slowik, J.G., Platt, S.M., Canonaco, F., Zotter, P., Wolf, R., Pieber, S.M., Bruns, E.A., Crippa, M., Ciarelli, G., Piazzalunga, A., Schwikowski, M., Abbaszade, G., Schnelle-Kreis, J., Zimmermann, R., An, Z.S., Szidat, S., Baltensperger, U., El Haddad, I., Prevot, A.S.H., 2014. High secondary aerosol contribution to particulate pollution during haze events in China. Nature 514, 218–222. https://doi.org/10.1038/nature13774.

Huang, X.Y., Zhang, Y.L., Yang, W.Q., Huang, Z.Z., Wang, Y.J., Zhang, Z., He, Q.F., Lü, S.J., Huang, Z.H., Bi, X.H., Wang, X.M., 2017. Effect of traffic restriction on reducing ambient volatile organic compounds (VOCs): observation-based evaluation during a traffic restriction drill in GuangzhouChina. Atmospheric Environment 161, 61–70. https://doi.org/10.1016/j.atmosenv.2017.04.035.

Huang, X.Y., Zhang, Y.L., Wang, Y.J., Ou, Y.B., Chen, D.H., Pei, C.L., Huang, Z.Z., Zhang, Z., Liu, T.Y., Luo, S.L., Huang, X.Q., Song, W., Ding, X., Shao, M., Zou, S.C., Wang, X.M., 2020. Evaluating the effectiveness of multiple emission control measures on reducing volatile organic compounds in ambient air based on observational data: a case study during the 2010 Guangzhou Asian games. Sci. Total Environ. 723, 138171. https://doi.org/10.1016/j.scitotenv.2020.138171.

Huang, X., Ding, A.J., Gao, J., Zheng, B., Zhou, D.R., Qi, X.M., Tang, R., Wang, J.P., Ren, C.H., Nie, W., Chi, X.G., Xu, Z., Chen, L.D., Li, Y.Y., Che, F., Pang, N.N., Wang, H.K., Tong, D., Qin, W., Cheng, W., Liu, W.J., Fu, Q.Y., Liu, B.X., Chai, F.H., Davis, S.J., Zhang, Q., He, K.B., 2021. Enhanced secondary pollution offset reduction of primary emissions during COVID-19 lockdown in China. National Science Review 8 (2), nwaa137. https://doi.org/10.1093/nsr/nwaa137.

Hui, L.R., Liu, X.G., Tan, Q.W., Feng, M., An, J., Qu, Y., Zhang, Y., Cheng, N., 2019. VOC characteristics, sources and contributions to SOA formation during haze events in WuhanCentral China. Science of The Total Environment 650, 2624–2639. https://doi.org/10.1016/j.scitotenv.2018.10.029.

Jia, H.H., Huo, J.T., Fu, Q.Y., Duan, Y.S., Lin, Y.F., Jin, X.D., Hu, X., Cheng, J.P., 2020. Insights into chemical composition, abatement mechanisms and regional transport of atmospheric pollutants in the Yangtze River Delta region, China during the COVID-19 outbreak control period. Environ. Pollut. 267, 115612. https://doi.org/10.1016/j.envpol.2020.115612.

Jin, X.M., Holloway, T., 2015. Spatial and temporal variability of ozone sensitivity over China observed from the ozone monitoring instrument. J. Geophys. Res.-Atmos. 120 (14), 7229–7246. https://doi.org/10.1002/2015JD023250.

Lal, P., Kumar, A., Kumar, S., Kumari, S., Saikia, P., Dayanandan, A., Adhikari, D., Khan, M.L., 2020. The dark cloud with a silver lining: assessing the impact of the SARS COVID-19 pandemic on the global environment. Sci. Total Environ. 732, 139297. https://doi.org/10.1016/j.scitotenv.2020.139297.

Li, J., Xie, S.D., Zeng, L.M., Li, L.Y., Li, Y.Q., Wu, R.R., 2015. Characterization of ambient volatile organic compounds and their sources in Beijing, before, during, and after Asia-Pacific economic cooperation China 2014. Atmos. Chem. Phys. 15, 7945–7959. https://doi.org/10.5194/acp-15-7945-2015.

Li, J., Wu, R.R., Li, Y.Q., Hao, Y.F., Xie, S.D., Zeng, L.M., 2016. Effects of rigorous emission controls on reducing ambient volatile organic compounds in BeijingChina. Science of the Total Environment 557, 531–541. https://doi.org/10.1016/j.scitotenv.2016.03.140.

Li, M., Zhang, Q., Kurokawa, J.-I., Woo, J.-H., He, K., Lu, Z., Ohara, T., Song, Y., Streets, D.G., Carmichael, G.R., Cheng, Y., Hong, C., Huo, H., Jiang, X., Kang, S., Liu, F., Su, H., Zheng, B., 2017. MIX: a mosaic Asian anthropogenic emission inventory under the international collaboration framework of the MICS-Asia and HTAP. Atmos. Chem. Phys. 17, 935–963. https://doi.org/10.5194/acp-17-935-2017.

Li, K., Jacob, D.J., Shen, L., Lu, X., De Smedt, I., Liao, H., 2020a. Increases in surface ozone pollution in China from 2013 to 2019: anthropogenic and meteorological influences. Atmos. Chem. Phys. 20, 11423–11433. https://doi.org/10.5194/acp-20-11423-2020.

Li, L., Li, Q., Huang, L., Wang, Q., Zhu, A., Xu, J., Liu, Z., Li, H., Shi, L., Li, R., Azari, M., Wang, Y., Zhang, X., Liu, Z., Zhu, Y., Zhang, K., Xue, S., Ooi, M.C.G., Zhang, D., Chan, A., 2020b. Air quality changes during the COVID-19 lockdown over the Yangtze River Delta region: an insight into the impact of human activity pattern changes on air pollution variation. Sci. Total Environ. 732, 139282. https://doi.org/10.1016/j.scitotenv.2020.139282.

Li, Y., Yan, Y., Hu, D., Li, Z., Hao, A., Li, R., Wang, C., Xu, Y., Cao, J., Liu, Z., Peng, L., 2020c. Source apportionment of atmospheric volatile aromatic compounds (BTEX) by stable carbon isotope analysis: a case study during heating period in Taiyuan, northern China. Atmos. Environ. 225, 117369. https://doi.org/10.1016/j.atmosenv.2020.117369.

Lian, X., Huang, J., Huang, R., Liu, C., Wang, L., Zhang, T., 2020. Impact of city lockdown on the air quality of COVID-19-hit of Wuhan city. Sci. Total Environ. 742, 140556. https://doi.org/10.1016/j.scitotenv.2020.140556.

Lim, Y.B., Ziemann, P.J., 2009. Effects of molecular structure on aerosol yields from OH radical-initiated reactions of linear, branched, and cyclic alkanes in the presence of NOx. Environ. Sci. Technol. 43, 2328–2334. https://doi.org/10.1021/es803389s.

Liu, Y., Shao, M., Fu, L.L., Lu, S.H., Zeng, L.M., Tang, D.G., 2008. Source profiles of volatile organic compounds (VOCs) measured in China: part I. Atmos. Environ. 42 (25), 6247–6260. https://doi.org/10.1016/j.atmosenv.2008.01.070.

Liu, H., Wang, X., Zhang, J., He, K., Wu, Y., Xu, J., 2013. Emission controls and changes in air quality in Guangzhou during the asian games. Atmos. Environ. 76, 81–93. https://doi.org/10.1016/j.atmosenv.2012.08.004.

Liu, K., Zhang, C., Cheng, Y., Liu, C., Zhang, H., Zhang, G., Sun, X., Mu, Y., 2015. Serious BTEX pollution in rural area of the North China plain during winter season. J. Environ. Sci. 30, 186–190. https://doi.org/10.1016/j.jes.2014.05.056.

Liu, Z.C., Li, N., Wang, N., 2016. Characterization and source identification of ambient VOCs in JinanChina. Air Quality, Atmosphere & Health 9 (3), 285–291. https://doi.org/10.1007/s11869-015-0339-2.

Liu, C.T., Ma, Z.B., Mu, Y.J., Liu, J.F., Zhang, C.L., Zhang, Y.Y., Liu, P.F., Zhang, H.X., 2017. The levels, variation characteristics, and sources of atmospheric non-methane hydrocarbon compounds during wintertime in BeijingChina. Atmospheric Chemistry and Physics 17, 10633–10649. https://doi.org/10.5194/acp-17-10633-2017.

Liu, Y., Song, M., Liu, X., Zhang, Y., Hui, L., Kong, L., Zhang, Y., Zhang, C., Qu, Y., An, J., Ma, D., Tan, Q., Feng, M., 2020. Characterization and sources of volatile organic compounds (VOCs) and their related changes during ozone pollution days in 2016 in BeijingChina. Environmental Pollution 257, 113599. https://doi.org/10.1016/j.envpol.2019.113599.

Lu, X., Zhang, L., Wang, X.L., Gao, M., Li, K., Zhang, Y.Z., Yue, X., Zhang, Y.H., 2020. Rapid increases in warm-season surface ozone and resulting health impact over China since 2013. Environ. Sci. Technol. Lett. https://doi.org/10.1021/acs.estlett.0c00171.

Lv, Z.F., Wang, X.T., Deng, F.Y., Ying, Q., Archibald, A.T., Jones, R.L., Ding, Y., Cheng, Y., Fu, M.L., Liu, Y., Man, H.Y., Xue, Z.G., He, K.B., Hao, J.M., Liu, H., 2020. Source-receptor relationship revealed by the halted traffic and aggravated haze in Beijing during the COVID-19 lockdown. Environ. Sci. Technol. 54 (24), 15660–15670. https://doi.org/10.1021/acs.est.0c04941.

Marlier, M.E., Xing, J., Zhu, Y., Wang, S., 2020. Impacts of COVID-19 response actions on air quality in China. Environ. Res. Commun. 2, 075003. https://doi.org/10.1088/2515-7620/aba425.

McCarthy, M.C., Aklilu, Y.-A., Brown, S.G., Lyder, D.A., 2013. Source apportionment of volatile organic compounds measured in EdmontonAlberta. Atmospheric Environment 81, 504–516. https://doi.org/10.1016/j.atmosenv.2013.09.016.

Miyazaki, K., Bowman, K., Sekiya, T., Jiang, Z., Chen, X., Eskes, H., Ru, M., Zhang, Y., Shindell, D., 2020. Air quality response in China linked to the 2019 novel coronavirus (COVID-19) lockdown. Geophys. Res. Lett. 47, e2020GL089252. https://doi.org/10.1029/2020GL089252.

Monteiro, A., Russo, M., Gama, C., Lopes, M., Borrego, C., 2018. How economic crisis influence air quality over Portugal (Lisbon and Porto)? Atmos. Pollut. Res. 9 (3), 439–445. https://doi.org/10.1016/j.apr.2017.11.009.

Moreira dos Santos, C.Y., de Almeida Azevedo, D., de Aquino Neto, F.R., 2004. Atmospheric distribution of organic compounds from urban areas near a coal-fired power station. Atmos. Environ. 38, 1247–1257. https://doi.org/10.1016/j.atmosenv.2003.11.026.

Ng, N.L., Kroll, J.H., Chan, A.W.H., Chhabra, P.S., Flagan, R.C., Seinfeld, J.H., 2007. Secondary organic aerosol formation from m-xylene, toluene, and benzene. Atmos. Chem. Phys. 7, 3909–3922. https://doi.org/10.5194/acp-7-3909-2007.

O'Dowd, C.D., Aalto, P., Hameri, K., Kulmala, M., Hoffmann, T., 2002. Aerosol formation - atmospheric particles from organic vapours. Nature 416, 497–498.. https://doi.org/10.1038/416497a.

Odum, J.R., Jungkamp, T.P.W., Griffin, R.J., Flagan, R.C., Seinfeld, J.H., 1997. The atmospheric aerosol-forming potential of whole gasoline vapor. Science 276, 96–99.. https://doi.org/10.1126/science.276.5309.96.

Ou, J., Guo, H., Zheng, J., Cheung, K., Louie, P.K.K., Ling, Z., Wang, D., 2015. Concentrations and sources of hydrocarbons (NMHCs) from 2005 to 2013 in Hong Kong: a multi-year real-time data analysis. Atmos. Environ. 103, 196–206. https://doi.org/10.1016/j.atmosenv.2014.12.048.

Pei, Z.P., Han, G., Ma, X., Su, H., Gong, W., 2020. Response of major air pollutants to COVID-19 lockdowns in China. Science of the Total Environment 743, 140879. https://doi.org/10.1016/j.scitotenv.2020.140879.

Pei, C.L., Mu, J.S., Zhang, Y.N., Shen, H.Q., Chen, Y.R., Huang, J.S., Ding, H.R., Li, C.L., 2021. Source apportionment of ozone pollution in Guangzhou: case study with the application of Lagrangian photochemical trajectory model. Environmental Sciences (in Chinese) 42 (4), 1615–1625. https://doi.org/10.13227/j.hjkx.202009058.

Qi, J., Mo, Z., Yuan, B., Huang, S., Huangfu, Y., Wang, Z., Li, X., Yang, S., Wang, W., Zhao, Y., Wang, X., Wang, W., Liu, K., Shao, M., 2021. An observation approach in evaluation of ozone production to precursor changes during the COVID-19 lockdown. Atmos. Environ. 262, 118618. https://doi.org/10.1016/j.atmosenv.2021.118618.

Sato, K., Takami, A., Isozaki, T., Hikida, T., Shimono, A., Imamura, T., 2010. Mass spectrometric study of secondary organic aerosol formed from the photo-oxidation of aromatic hydrocarbons. Atmos. Environ. 44, 1080–1087. https://doi.org/10.1016/j.atmosenv.2009.12.013.

Shao, P., An, J., Xin, J., Wu, F., Wang, J., Ji, D., Wang, Y., 2016. Source apportionment of VOCs and the contribution to photochemical ozone formation during summer in the typical industrial area in the Yangtze River Delta, China. Atmospheric Research 176 (Supplement C), 64–74. https://doi.org/10.1016/j.atmosres.2016.02.015.

Siciliano, B., Dantas, G., da Silva, C.M., Arbilla, G., 2020. Increased ozone levels during the COVID-19 lockdown: analysis for the city of Rio de JaneiroBrazil. Science of The Total Environment 737, 139765. https://doi.org/10.1016/j.scitotenv.2020.139765.

Song, Y., Shao, M., Liu, Y., Lu, S.H., Kuster, W., Goldan, P., Xie, S.D., 2007. Source apportionment of ambient volatile organic compounds in Beijing. Environ. Sci. Technol. 41 (12), 4348–4353. https://doi.org/10.1021/es0625982.

Speight, J.G., 2015. Liquid fuels from natural gas. In: Lee, S., Speight, J.G., Loyalka, S.K. (Eds.), Handbook of Alternative Fuel Technologies, second ed Taylor and Francis Group, LLC, CRC Press, pp. 157–178.

Tang, J.H., Chan, L.Y., Chan, C.Y., Li, Y.S., Chang, C.C., Wang, X.M., Zou, S.C., Barletta, B., Blake, D.R., Wu, D., 2008. Implications of changing urban and rural emissions on non-methane hydrocarbons in the Pearl River Delta region of China. Atmos. Environ. 42 (16), 3780–3794. https://doi.org/10.1016/j.atmosenv.2007.12.069.

Tie, X., Geng, F., Guenther, A., Cao, J., Greenberg, J., Zhang, R., Apel, E., Li, G., Weinheimer, A., Chen, J., Cai, C., 2013. Megacity impacts on regional ozone formation: observations and WRF-chem modeling for the MIRAGE-Shanghai field campaign. Atmos. Chem. Phys. 13, 5655–5669. https://doi.org/10.5194/acp-13-5655-2013.

Venter, Z.S., Aunan, K., Chowdhury, S., Lelieveld, J., 2020. COVID-19 lockdowns cause global air pollution declines. Proc. Natl. Acad. Sci. U. S. A. 117, 18984–18990. https://doi.org/10.1073/pnas.2006853117.

Wang, X.Y., Zhang, R.H., 2020. How did air pollution change during the COVID-19 outbreak in China? Bulletin of the American Meteorological Society 101 (10). https://doi.org/10.1175/BAMS-D-20-0102.1.

Wang, T., Cheung, T.F., Li, Y.S., Yu, X.M., Blake, D.R., 2002a. Emission characteristics of CO, NOx, SO2 and indications of biomass burning observed at a rural site in eastern China. J. Geophys. Res.-Atmos. 107, D12. https://doi.org/10.1029/2001JD000724.

Wang, X.M., Sheng, G.Y., Fu, J.M., Chan, C.Y., Lee, S.G., Chan, L.Y., Wang, Z.S., 2002. Urban roadside aromatic hydrocarbons in three cities of the Pearl River Delta, People's Republic of China. Atmospheric Environment 36 (33), 5141–5148. https://doi.org/10.1016/S1352-2310(02)00640-4.

Wang, H.L., Qiao, Y.Z., Chen, C.H., Lu, J., Dai, H.X., Qiao, L.P., Lou, S.R., Huang, C., Li, L., Jing, S.G., Wu, J.P., 2014. Source profiles and chemical reactivity of volatile organic compounds from solvent use in ShanghaiChina. Aerosol and Air Quality Research 14, 301–310. https://doi.org/10.4209/aaqr.2013.03.0064.

Wang, L., Li, M., Yu, S., Chen, X., Li, Z., Zhang, Y., Jiang, L., Xia, Y., Li, J., Liu, W., Li, P., Lichtfouse, E., Rosenfeld, D., Seinfeld, J.H., 2020a. Unexpected rise of ozone in urban and rural areas, and sulfur dioxide in rural areas during the coronavirus city lockdown in Hangzhou, China: implications for air quality. Environ. Chem. Lett. 18 (5), 1713–1723. https://doi.org/10.1007/s10311-020-01028-3.

Wang, P.F., Chen, K.Y., Zhu, S.Q., Wang, P., Zhang, H.L., 2020b. Severe air pollution events not avoided by reduced anthropogenic activities during COVID-19 outbreak. Resour. Conserv. Recycl. 158 (104814), 2020b. https://doi.org/10.1016/j.resconrec.2020.104814.

Wang, Y., Yuan, Y., Wang, Q., Liu, C., Zhi, Q., Cao, J., 2020c. Changes in air quality related to the control of coronavirus in China: implications for traffic and industrial emissions. Sci. Total Environ. 731, 139133. https://doi.org/10.1016/j.scitotenv.2020.139133.

Wang, J., Zhang, Y.L., Wu, Z.F., Luo, S.L., Song, W., Wang, X.M., 2021a. Ozone episodes during and after the 2018 chinese National day Holidays in Guangzhou: implications for the control of precursor VOCs. J. Environ. Sci. https://doi.org/10.1016/j.jes.2021.09.009.

Wang, M., Lu, S., Shao, M., Zeng, L., Zheng, J., Xie, F., Lin, H., Hu, K., Lu, X., 2021b. Impact of COVID-19 lockdown on ambient levels and sources of volatile organic compounds (VOCs) in NanjingChina. Science of Total Environment 757, 143823. https://doi.org/10.1016/j.scitotenv.2020.143823.

Wang, N., Xu, J.W., Pei, C.L., Tang, R., Zhou, D.R., Chen, Y.N., Li, M., Deng, X.J., Deng, T., Hang, X., Ding, A.J., 2021c. Air quality during COVID-19 lockdown in the Yangtze River Delta and the Pearl River Delta: two different responsive mechanisms to emission reductions in China. Environ. Sci. Technol. 55 (9), 5721–5730. https://doi.org/10.1021/acs.est.0c08383.

Wang, P., Shen, J.Y., Xia, M., Sun, S., Zhang, Y.L., Zhang, H.L., Wang, X.M., 2021d. Unexpected enhancement of ozone exposure and health risks during National day in China. Atmos. Chem. Phys. https://doi.org/10.5194/acp-21-10347-2021.

Wang, S.Y., Zhang, Y.L., Ma, J.L., Zhu, S.Q., Shen, J.Y., Wang, P., Zhang, H.L., 2021e. Responses of decline in air pollution and recovery associated with COVID-19 lockdown in the Pearl River Delta. Sci. Total Environ. 756, 143868. https://doi.org/10.1016/j.scitotenv.2020.143868.

Watson, J.G., Chow, J.C., Fujita, E.M., 2001. Review of volatile organic compound source apportionment by chemical mass balance. Atmos. Environ. 35 (9), 1567–1584. https://doi.org/10.1016/S1352-2310(00)00461-1.

Wu, R.R., Xie, S.D., 2017. Spatial distribution of ozone formation in China derived from emissions of speciated volatile organic compounds. Environ. Sci. Technol. 51 (5), 2574–2583. https://doi.org/10.1021/acs.est.6b03634.

Wu, F., Yu, Y., Sun, J., Zhang, J., Wang, J., Tang, G., Wang, Y., 2016. Characteristics, source apportionment and reactivity of ambient volatile organic compounds at Dinghu Mountain in Guangdong ProvinceChina. Science of The Total Environment 548, 347–359. https://doi.org/10.1016/j.scitotenv.2015.11.069.

Wu, Z.F., Zhang, Y.L., He, J.J., Chen, H.Z., Huang, X.L., Wang, Y.J., Yu, X., Yang, W.Q., Zhang, R.Q., Zhu, M., Li, S., Fang, H., Zhang, Z., Wang, X.M., 2020. Dramatic increase in reactive volatile organic compound (VOC) emissions from ships at berth after implementing the fuel switch policy in the Pearl River Delta Emission Control Area. Atmos. Chem. Phys. 20, 1887–1900. https://doi.org/10.5194/acp-20-1887-2020.

Xu, R.G., Tang, G.Q., Wang, Y.S., Tie, X.X., 2016. Analysis of a long-term measurement of air pollutants (2007–2011) in North China plain (NCP): impact of emission reduction during the Beijing olympic games. Chemosphere 159, 647–658. https://doi.org/10.1016/j.chemosphere.2016.06.025.

Xue, Y.F., Zhou, Z., Nie, T., Wang, K., Nie, L., Pan, T., Wu, X.Q., Tian, H.Z., Zhong, L.H., Li, J., Liu, H.J., Liu, S.H., Shao, P.Y., 2016. Trends of multiple air pollutants emissions from residential coal combustion in Beijing and its implication on improving air quality for control measures. Atmos. Environ. 142, 303–312. https://doi.org/10.1016/j.atmosenv.2016.08.004.

Yang, W.Q., Zhang, Y.L., Wang, X.M., Li, S., Zhu, M., Yu, Q.Q., Li, G.H., Huang, Z.H., Zhang, H.N., Wu, Z.F., Song, W., Tan, J.H., Shao, M., 2018. Volatile organic compounds at a rural site in Beijing: influence of temporary emission control and wintertime heating. Atmos. Chem. Phys. 18, 12663–12682. https://doi.org/10.5194/acp-18-12663-2018.

Yuan, B., Shao, M., Lu, S.H., Wang, B., 2010. Source profiles of volatile organic compounds associated with solvent use in BeijingChina. Atmospheric Environment 44 (15), 1919–1926. https://doi.org/10.1016/j.atmosenv.2010.02.014.

Zhang, Y.L., Wang, X.M., Blake, D.R., Li, L.F., Zhang, Z., Wang, S.Y., Guo, H., Lee, F.S.C., Gao, B., Chan, L.Y., Wu, D., Rowland, F.S., 2012. Aromatic hydrocarbons as ozone precursors before and after outbreak of the 2008 financial crisis in the Pearl River Delta region, South China. J. Geophys. Res.-Atmos. 117, 16. https://doi.org/10.1029/2011JD017356.

Zhang, Y.L., Wang, X.M., Zhang, Z., Lu, S., Shao, M., Lee, F.S.C., Yu, J., 2013. Species profiles and normalized reactivity of volatile organic compounds from gasoline evaporation in China. Atmos. Environ. 79, 110–118. https://doi.org/10.1016/j.atmosenv.2013.06.029.

Zhang, J.K., Sun, Y., Liu, Z.R., Ji, D.S., Hu, B., Liu, Q., Wang, Y.S., 2014. Characterization of submicron aerosols during a month of serious pollution in Beijing, 2013. Atmos. Chem. Phys. 14, 2887–2903. https://doi.org/10.5194/acp-14-2887-2014.

Zhang, Z., Wang, X.M., Zhang, Y.L., Lü, S., Huang, Z., Huang, X., Wang, Y., 2015. Ambient air benzene at background sites in China's most developed coastal regions: exposure levels, source implications and health risks. Sci. Total Environ. 511, 792–800. https://doi.org/10.1016/j.scitotenv.2015.01.003.

Zhang, Y.L., Yang, W.Q., Simpson, I., Huang, X.Y., Yu, J.Z., Huang, Z.H., Wang, Z.Y., Zhang, Z., Liu, D., Huang, Z.Z., Wang, Y.J., Pei, C.L., Shao, M., Blake, D.R., Zheng, J.Y., Huang, Z.J., Wang, X.M., 2018. Decadal changes in emissions of volatile organic compounds (VOCs) from on-road vehicles with intensified automobile pollution control: case study in a busy urban tunnel in South China. Environ. Pollut. 233, 806–819. https://doi.org/10.1016/j.envpol.2017.10.133.

Zhang, G., Xu, H., Wang, H., Xue, L., He, J., Xu, W., Qi, B., Du, R., Liu, C., Li, Z., Gui, K., Jiang, W., Liang, L., Yan, Y., Meng, X., 2020. Exploring the inconsistent variations in atmospheric primary and secondary pollutants during the 2016 G20 summit in Hangzhou, China: implications from observations and models. Atmos. Chem. Phys. 20, 5391–5403. https://doi.org/10.5194/acp-20-5391-2020.

Zhang, Y., Xue, L., Carter, W.P.L., Pei, C., Chen, T., Mu, J., Wang, Y., Zhang, Q., Wang, W., 2021. Development of ozone reactivity scales for volatile organic compounds in a Chinese megacity. Atmos. Chem. Phys. 14, 11053–11068. https://doi.org/10.5194/acp-21-11053-2021.

Zheng, J.Y., Yu, Y.F., Mo, Z.W., Zhang, Z., Wang, X.M., Yin, S.S., Peng, K., Yang, Y., Feng, X.Q., Cai, H.H., 2013. Industrial sector-based volatile organic compound (VOC) source profiles measured in manufacturing facilities in the Pearl River DeltaChina. Science of the Total Environment 456–457, 127–136. https://doi.org/10.1016/j.scitotenv.2013.03.055.